MOLECULAR AND CELLULAR BIOLOGY, Jan. 2002, p. 270–285 Vol. 22, No. 1
0270-7306/02/$04.00+0 DOI: 10.1128/MCB.22.1.270–285.2002
Copyright © 2002, American Society for Microbiology. All Rights Reserved.

Erk5 Participates in Neuregulin Signal Transduction and Is Constitutively Active in Breast Cancer Cells Overexpressing ErbB2

Azucena Esparís-Ogando,[1] Elena Díaz-Rodríguez,[1] Juan Carlos Montero,[1] Laura Yuste,[1] Piero Crespo,[2] and Atanasio Pandiella[1]*

Instituto de Microbiología Bioquímica and Centro de Investigación del Cáncer, Consejo Superior de Investigaciones Científicas, Universidad de Salamanca, Salamanca,[1] and Instituto Investigaciones Biomédicas, Madrid,[2] Spain

Received 11 June 2001/Accepted 8 October 2001

The four receptor tyrosine kinases of the ErbB family play essential roles in several physiological processes and have also been implicated in tumor generation and/or progression. Activation of ErbB1/EGFR is mainly triggered by epidermal growth factor (EGF) and other related ligands, while activation of ErbB2, ErbB3, and ErbB4 receptors occurs by binding to another set of EGF-like ligands termed neuregulins (NRGs). Here we show that the Erk5 mitogen-activated protein kinase (MAPK) pathway participates in NRG signal transduction. In MCF7 cells, NRG activated Erk5 in a time- and dose-dependent fashion. The action of NRG on Erk5 was dependent on the kinase activity of ErbB receptors but was independent of Ras. Expression in MCF7 cells of a dominant negative form of Erk5 resulted in a significant decrease in NRG-induced proliferation of MCF7 cells. Analysis of Erk5 in several human tumor cell lines indicated that a constitutively active form of this kinase was present in the BT474 and SKBR3 cell lines, which also expressed activated forms of ErbB2, ErbB3, and ErbB4. Treatments aimed at decreasing the activity of these receptors caused Erk5 inactivation, indicating that the active form of Erk5 present in BT474 and SKBR3 cells was due to a persistent positive stimulus originating at the ErbB receptors. In BT474 cells expression of the dominant negative form of Erk5 resulted in reduced proliferation, indicating that in these cells Erk5 was also involved in the control of proliferation. Taken together, these results suggest that Erk5 may play a role in the regulation of cell proliferation by NRG receptors and indicate that constitutively active NRG receptors may induce proliferative responses in cancer cells through this MAPK pathway.

Receptor tyrosine kinases of the ErbB family play essential roles in several physiological processes, such as cell growth (11, 36, 66), differentiation, and tissue development (8, 55, 61), and have been implicated in pathological processes, such as tumor generation and/or progression (36, 66). This family comprises four structurally related transmembrane receptors, the epidermal growth factor (EGF) receptor (EGFR or ErbB1/HER1), ErbB2 (neu/HER2), ErbB3 (HER3), and ErbB4 (HER4) (36, 66). Activation of ErbB receptors may occur by ligand binding (67, 68) or by overexpression of the receptor (36, 57), the latter mechanism being particularly relevant in certain pathologic instances such as cancer (30, 62–64). Ligand-mediated activation of ErbB receptors occurs by interaction of the ectodomain of these receptors with specific members of the EGF family of ligands (11, 48). This family includes EGF, transforming growth factor α, amphiregulin, betacellulin, and epiregulin, which preferentially bind to and activate the EGFR (3, 48, 65). A second group of EGF-like ligands, the neuregulins (NRGs), bind to ErbB3 and ErbB4 (6, 38, 53). Ligand-induced activation of ErbB receptors is complex and often includes oligomeric interactions between different ErbB receptors (19, 54). Thus, upon ligand binding, ErbB receptors oligomerize and this results in transphosphorylation of the receptors on tyrosine residues. While ligand-induced homooligomerization of EGFR or ErbB4 results in its activation, heterooligomerization is expected to play a major role in the function of ErbB3 and ErbB2. In fact, ErbB3 contains an inefficient kinase activity in its intracellular domain that would prevent activation of ErbB3 homooligomers (32). On the other hand, ErbB2 does not bind any EGF family ligand with enough affinity, thus preventing its activation by ligands (65). Cooperation between these receptors has been demonstrated in cell lines expressing ErbB2 and ErbB3 (29, 50, 52, 69). In these models, signal transduction occurs by the combined action of ErbB3 acting as a receptor for the ligand that is then presented to ErbB2, which acts as a signal transducer and phosphorylates ErbB3 in heterodimeric ErbB2-ErbB3 complexes.

Tyrosine phosphorylation of specific residues within the intracellular domain of the receptors results in the binding of signaling molecules with enzymatic activity or adaptor molecules that allow activation of specific intracellular targets (68). Important downstream pathways that are activated by these receptors and have been linked to the regulation of cell proliferation are the mitogen-activated protein kinase (MAPK) routes (58, 70). MAPK routes are characteristically organized into a three-kinase module that includes a MAPK; the upstream kinase MEK or MKK, which phosphorylates and activates the MAPK; and the MEK kinase, which is responsible for the activation of MEK (26). Three major MAPK pathways in

* Corresponding author. Mailing address: Instituto de Microbiología Bioquímica, Edificio Departamental, Ave. del Campo Charro s/n, 37007, Salamanca, Spain. Phone: 34-923-120561. Fax: 34-923-224876. E-mail: atanasio@usal.es.

Downloaded from http://mcb.asm.org/ on October 23, 2019 by guest

mammals have been described (13). The extracellular signal-regulated kinase 1 (Erk1) and Erk2 (Erk1/2) route is activated by receptors for polypeptide growth factors (26), by G protein-coupled receptors (31), or by direct stimulation of intracellular pathways such as the protein kinase C messenger system (59). Growth factor receptor stimulation results in activation of the Ras pathway, which then triggers the activity of Raf kinases, which phosphorylate and activate the dual-specificity MEKs responsible for the tyrosine and threonine phosphorylation and activation of Erk1/2 (46, 60). Erks then phosphorylate cytoplasmic substrates (26, 70) and are also translocated to the nucleus (27, 44). As a result of Erk translocation, several nuclear proteins, such as transcription factors (37, 58, 70) or other structural proteins (75), are phosphorylated, and this causes induction of genes that participate in proliferative and differentiative responses. The two other MAPK routes, the p38 and Jun N-terminal kinase pathways, are mainly triggered by cytokine and stress stimuli (37, 56). Although they appear to be regulated by analogous stimuli, their upstream activating kinases are, however, different (37, 70). In several different cellular models, all of these MAPK routes have been shown to be triggered by neuregulin (NRG) receptors (18, 24, 28, 53). Use of specific inhibitors of the Erk1/2 pathway has indicated that this route participates in NRG-induced proliferation of breast cancer cells (24). In contrast, p38 activation has been reported to result in an apoptotic response (17, 18).

Another MAPK route, the Big MAPK-1/Erk5 kinase pathway, has also been implicated in proliferative responses (21, 41). This pathway has been shown to be activated by EGF (39, 41) and differentiative factors such as NGF (39) and also participates in cellular responses to hyperosmolarity and oxidative and mechanical stresses (1, 2, 73). The intracellular cascades leading to Erk5 activation, as well as the targets of this kinase, are being uncovered. Participation of the Ras/Raf pathway is still unclear. Thus, stimulation of the EGFR in HeLa cells led to Erk1/2 and Erk5 activation; however, expression of a dominant negative form of Ras prevented Erk1/2 activation, leaving unaffected the ability of EGF to induce Erk5 activation (41). In contrast, NGF- or EGF-induced Erk5 activation in PC12 cells is inhibited by the presence of dominant negative forms of Ras (39). Other studies on Erk5 activation have indicated that itinerant cytosolic tyrosine kinases such as c-Src may participate in Erk5 regulation (2).

More accepted are the identities of the Erk5 upstream activating kinases. Thus, the upstream dual-specificity kinase MEK5 has been shown to physically interact with Erk5 (74, 76), and constitutively active mutant forms of MEK5 selectively activate Erk5 but not other MAP kinases (40). Functional studies have also shown that a dominant negative form of MEK5 prevents serum-induced (40) and G protein-coupled receptor-mediated (45) Erk5 activation. Thus, these studies indicate that MEK5 may act as the immediately upstream Erk5-activating kinase. Studies on possible activators of MEK5 have identified the MEKK3 kinase as a possible regulator of MEK5 (14).

Here we have investigated whether the Erk5 pathway may be activated by NRG receptors. We show that NRG activates the Erk5 pathway in several cancer cell lines. Furthermore, lines overexpressing active forms of ErbB2, such as SKBR3 and BT474 breast cancer cells, do express constitutively active, dually phosphorylated Erk5. Expression in MCF7 cells of a dominant negative form of Erk5 resulted in a significant decrease in NRG-induced cell proliferation, indicating that this kinase participates in the transduction of signals that lead to cell duplication upon activation of NRG receptors.

MATERIALS AND METHODS

Reagents and immunochemicals. Cell culture media, sera, and G418 were purchased from GIBCO BRL (Gaithersburg, Md.). Protein A-Sepharose was from Amersham-Pharmacia (Piscataway, N.J.). Immobilon P membranes were from Millipore Corp. (Bedford, Mass.). U0126 was from Calbiochem. EGF was from Collaborative Research. DAPH (10) was generously provided by N. B. Lydon (Novartis Pharma, Basel, Switzerland). Other generic chemicals were purchased from Sigma Chemical Co., Roche Biochemicals, or Merck.

The anti-hemagglutinin (HA) monoclonal antibody was from BAbCO, and the anti-Shc antibody was from UBI. The mouse anti-phosphotyrosine, anti-c-Jun, and anti-phospho-Erk1/2 monoclonal antibodies, the rabbit polyclonal anti-Erk and anti-Ras antibodies, and the anti-ErbB antibodies used for immunoprecipitation were from Santa Cruz Biotechnology, as was the goat anti-Erk5 C-20 antibody. The Ab3 anti-ErbB2 antibody used for Western blotting was from Oncogene Science. The anti-HER2 ectodomain 4D5 monoclonal antibody was provided by Mark X. Sliwkowski (Genentech, San Francisco, Calif.). The 528 monoclonal antibody against the EGFR was generously provided by John Mendelsohn (M. D. Anderson Cancer Center, Houston, Tex.). The Cy3-conjugated secondary antibodies were from Jackson Immunoresearch. Horseradish peroxidase conjugates of anti-rabbit and anti-mouse immunoglobulin G were from Bio-Rad Laboratories (Cambridge, Mass.).

Cell culture and transfections. All cell lines were cultured at 37°C in a humidified atmosphere in the presence of 5% CO_2–95% air. Cells were grown in Dulbecco modified Eagle medium (DMEM) containing a high glucose concentration (4,500 mg/liter) and antibiotics (penicillin at 100 U/ml, streptomycin at 100 μg/ml) and supplemented with 5% (HeLa cells) or 10% (MCF7, BT474, SKBR3, NP9, NP29, NP31, A431, KB, and SKNBE cells) fetal bovine serum (FBS). The cell line NP18 was grown in RPMI medium containing antibiotics and 10% FBS.

Transfections of MCF7 or BT474 cells were performed with calcium phosphate, and clones were selected with G418. Single clones were analyzed for transfected-protein content by Western blotting with the anti-HA antibody (HA-Erk5^{AEF}) or the Ab-3 antibody (ErbB2).

To generate MCF7 cell lines that expressed HA-Erk5^{AEF} or RasN17 in a regulated manner, we used the tetracycline transactivator system. MCF7-Tet-Off cells (obtained either from R. Michalides [77] or from Clontech) were transfected with pTRE2-HA-Erk5^{AEF}, with pTRE2-RasN17, or with pTRE2 together with pBabe-Puro using Lipofectamine (Gibco-BRL). Clones were then selected with puromycin at 3 μg/ml, and the expression of the proteins was analyzed by Western blotting, comparing the amounts of HA-Erk5^{AEF} or RasN17 in the absence and presence of doxycycline at 0.1 to 1 μg/ml.

Generation of antibodies. Erk5-specific antiserum was raised in rabbits against the sequence NH_2-ESLQREIQWDSPML-COOH (residues 791 to 805), located at the C terminus of Erk5. A polyclonal anti-HA serum was obtained from rabbits immunized with the peptide NH_2-CYPYDVPDYAG-COOH. All of these antipeptide antibodies were purified by affinity chromatography using peptide-Sepharose columns.

The anti-pErk5 antibody was generated in rabbits against the sequence NH_2-HQYFMpTEpYVATRW-COOH (residues 213 to 225). The keyhole limpet hemocyanin-coupled peptide was injected into rabbits that were bled after the second booster. The sera were precleared of antibodies reacting against nonphosphorylated residues by three consecutive affinity purifications over a column of CNBr-agarose-HQYFMTEYVATRW. The last purification over this column gave rise to fractions whose A_{280} was below 0.1. Once depleted of antibodies reacting to the nonphosphorylated peptide, the serum was passed over a column prepared with the phosphorylated peptide. Fractions with an A_{280} greater than 0.8 were pooled and characterized by immunoprecipitation and Western blotting as shown in Fig. 1.

Plasmids and fusion proteins. HA-Erk5 was subcloned into the pCEFL mammalian expression vector. This is a modified version of the pCDNA3 vector that includes the elongation factor 1 promoter that controls the expression of an N-terminal HA tag after which the Erk5 cDNA is located (45). To generate a dominant negative form of Erk5, an *Eco*RI fragment from wild-type pCEFL-HA-Erk5 was subcloned into the *Eco*RI site of pCDNA3. Site-directed mutagenesis of the region containing the activating TEY microdomain (TEY to AEF)

Downloaded from http://mcb.asm.org/ on October 23, 2019 by guest

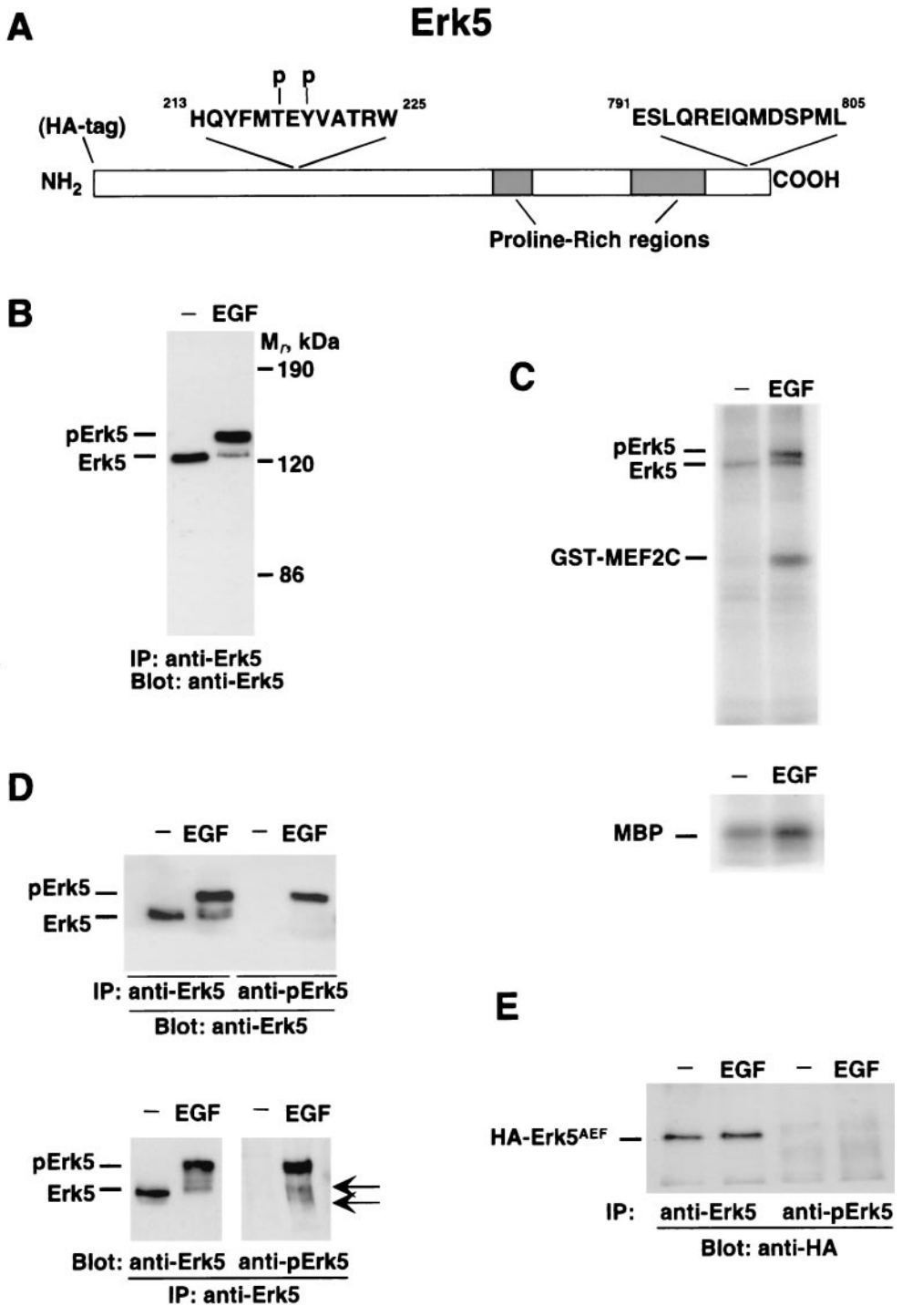

FIG. 1. Characterization of an antibody that recognizes active Erk5. (A) Representation of Erk5 indicating the epitopes against which the anti-Erk5 C terminus antibody and the anti-pErk5 antibody were generated. Also shown is the position of the HA epitope at the N-terminal end. (B) Change in mobility of Erk5 upon EGFR activation. HeLa cells were treated with EGF (10 nM) for 15 min, and then Erk5 was immunoprecipitated (IP) with the anti-Erk5 C terminus antibody, followed by Western blotting with the anti-Erk5 C-20 antibody. M_r, relative molecular weight. (C) In vitro kinase assays of Erk5 activation by EGF. HeLa cells were treated with EGF, and then lysates were precipitated with the anti-Erk5 C terminus antibody. Kinase reactions were carried out in the presence of MBP (bottom) or GST-MEF2C (top). (D) Recognition of activated Erk5 by the anti-pErk5 antibody. HeLa cells were stimulated with EGF, and lysates were immunoprecipitated with the anti-C terminus (anti-Erk5) or anti-pErk5 antibody and then subjected to Western analysis with the anti-Erk5 C-20 antibody (top). Another set of anti-Erk5 immunoprecipitates was blotted with the C-20 or anti-pErk5 antibody (bottom). The positions of two bands recognized only in EGF-treated samples by the anti-pErk5 antibody are shown by the arrows. (E) Failure of the anti-pErk5 antibody to recognize a mutant Erk5 form that is unable to undergo dual phosphorylation at the activation site. The mutant protein (HA-Erk5^{AEF}), tagged at the N terminus with an HA epitope, was transfected into HeLa cells. Where indicated, cells were treated with EGF and lysates were immunoprecipitated with the anti-Erk5 or anti-pErk5 antibody. Western blots were then probed with the anti-HA antibody.

Downloaded from http://mcb.asm.org/ on October 23, 2019 by guest

was performed by using standard procedures (5). After verification by sequencing, the *Eco*RI fragment was again placed into pCEFL-HA-Erk5 to generate pCEFL-HA-Erk5^{AEF}. The dominant negative form of Ras (RasN17) was also subcloned into the pCEFL vector. The human ErbB2 cDNA (provided by M. Kraus, Istituto Europeo di Oncologia, Milan, Italy) was subcloned into the *Xho*I site of pCDNA3 to generate the pCDNA3-ErbB2 mammalian expression plasmid. To generate inducible clones of MCF7 cells, HA-Erk5^{AEF} was subcloned into *Bam*HI/*Not*I sites of the pTRE2 vector (Clontech Laboratories). For retrovirus production, HA-Erk5^{AEF} was subcloned into the *Bam*HI/*Sal*I sites of the pRev-TetOff plasmid (Clontech Laboratories) or into the pLZR-IRES-GFP vector (provided by A. Bernad, Centro Nacional de Biotecnologia, Madrid, Spain). The dominant negative form of Ras (RasN17) was subcloned into the *Bam*HI/*Not*I sites of the pTRE2 vector or into the *Bam*HI/*Sal*I sites of pLZR-IRES-GFP.

A glutathione *S*-transferase (GST)-MEF2C fusion protein containing full-length MEF2C was generated by PCR amplification of a fragment using His-MEF2C (provided by J. D. Lee, Scripps Institute, La Jolla, Calif.) as a template and the oligonucleotides MEF2C 5′ (5′-GGGAATTCGAGGATGTCGACCTGC-3′; an *Eco*RI site is underlined) and MEF2C 3′ (5′-CCAAGCTTGTCGCATGCGCTTGAC-3′; a *Hin*dIII site is underlined). Plasmids were transformed in *Escherichia coli* strain BL21 or JM101, and the bacteria were induced with 0.2 mM isopropyl-β-D-thiogalactopyranoside (IPTG) for 2 h at 37°C. Bacteria were lysed, and the fusion proteins were isolated from the lysate by glutathione-Sepharose or nickel affinity chromatography. The fusion proteins were eluted from the resin with reduced glutathione or imidazole, and the amount of protein was quantitated by sodium dodecyl sulfate-polyacrylamide gel electrophoresis (SDS-PAGE) using various amounts of bovine serum albumin (BSA) as standards. A GST-EGFR fusion protein that included the 301 COOH-terminal residues of the human EGFR was used to generate polyclonal anti-EGFR antibodies as previously described (22).

Retrovirus production and infection. For transient generation of retroviruses, 293T cells were plated in 60-mm-diameter dishes (1.8×10^6 cells in 3 ml of DMEM with 10% FBS) and allowed to attach overnight. Five minutes prior to transfection, 25 μM chloroquine was added to each plate. The transfection solution contained DNA (2.5 μg of pMD-G, 5 μg of pNGVL-MLV-gag-pol, 3 μg of retroviral vector [pLZR-HA-Erk5^{AEF}-IRES-GFP, pLZR-RasN17-IRES-GFP, or pLZR-IRES-GFP alone for the mock transfection]), 61 μl of 2 M $CaCl_2$, and double-distilled H_2O to 500 μl. After mixing, 0.5 ml of 2× HBS (pH 7.0) (5) was added and the solution was bubbled for 15 s. The HBS-DNA complex was then dropped onto cells. Eight hours later, the medium was replaced with fresh complete culture medium that, 24 to 32 h posttransfection, was again replaced with 3 ml of fresh virus-collecting medium. Twenty-four hours after the medium change, the supernatant from transfected cells was collected and centrifuged at $1,000 \times g$ for 5 min. Twenty-four hours before infection, MCF7 or BT474 cells were plated at 25,000 per well in 24-well plates and infected with viral supernatants containing Polybrene at 6 μg/ml. The following day, the medium was changed to overnight-infected MCF7 cells, and 12 h later, infected cells were incubated in DMEM with 0.1% FBS and 10 nM NRG or the indicated concentrations of FBS. Cell proliferation was analyzed by an MTT-based assay (53).

For stable production of retroviruses, PT67 packaging cells (Clontech Laboratories) were transfected with retroviral plasmid pRevTRE-HA-Erk5^{AEF} or pRevTRE (Clontech Laboratories) alone. Two days after transfection, cells were plated in selection medium containing hygromycin (300 μg/ml; Calbiochem). Retrovirus produced by stable packaging clones and pools were analyzed by infecting MCF7-Tet-Off cells with virus-containing medium complemented with Polybrene (4 μg/ml). Forty-eight hours postinfection, infected MCF7-Tet-Off cells were split in the presence or absence of doxycycline (10 ng/ml). Cells were analyzed for infected-protein content by Western blotting with an anti-HA antibody.

Immunoprecipitation and Western blotting. Cells were washed with phosphate-buffered saline (PBS) and lysed in ice-cold lysis buffer (140 mM NaCl, 10 mM EDTA, 10% glycerol, 1% Nonidet P-40, 20 mM Tris (pH 8.0), 1 mM pepstatin, aprotinin at 1 μg/ml, leupeptin at 1 μg/ml, 1 mM phenylmethylsulfonyl fluoride, 1 mM sodium orthovanadate). After the cells had been scraped from the dishes, samples were centrifuged at $10,000 \times g$ at 4°C for 10 min and supernatants were transferred to new tubes with the corresponding antibody and protein A-Sepharose. Immunoprecipitations were performed at 4°C for at least 2 h, and the immune complexes were recovered by a short centrifugation, followed by three washes with 1 ml of cold lysis buffer. Samples were then boiled in electrophoresis sample buffer and loaded onto SDS-PAGE gels. After transfer to polyvinylidene difluoride membranes, filters were blocked for 1 h in TBST (12) and then incubated for 2 to 16 h with the corresponding antibody. After being washed with TBST, filters were incubated with horseradish peroxidase-conjugated secondary antibodies for 30 min and bands were visualized by a luminol-based detection system with *p*-iodophenol enhancement (12).

Cell proliferation measurements. Subconfluent monolayer cultures were trypsinized, and cells were plated in 24-well plates to a density of 25,000 per well. Cultures were allowed to attach overnight before treatment with different concentrations of serum in the presence or absence of NRG (10 nM). Cell proliferation was analyzed every 2 or 3 days by an MTT-based assay as follows. The medium in each well was replaced with 250 μl of fresh medium containing MTT at 0.5 μg/μl and plates were returned to the incubator for 1 h. The medium-MTT was then removed, 500 μl of dimethyl sulfoxide was added to each well, and the plate was kept in agitation for 5 min in the dark to dissolve the MTT-formazan crystals. The absorbance of the samples was then recorded at 570 nm. Four wells were analyzed for each condition, and wells containing medium plus MTT but no cells were used as blanks. The results are presented as the mean ± the standard deviation (SD) of quadruplicates of a representative experiment that was repeated at least three times.

To measure proliferation in MCF7-HA-Erk5^{AEF}-Tet-Off cells, they were plated at 10,000 per well and cultured overnight in DMEM–10% FBS with or without doxycycline at 10 ng/ml. The next day (day 1 of culture), an MTT assay was performed and considered the starting point. Five days after plating, another MTT uptake assay was carried out and parallel cultures of cells were shifted to DMEM–0.1% FBS containing or not containing doxycycline and 10 nM NRG. At 4 (day 9 of culture) and 6 (day 11 of culture) days after the addition of NRG, the MTT uptake assay was performed as described above. In parallel, wells of cells being treated or not being treated with doxycycline were lysed at the different times at which the MTT assays were performed and HA-Erk5^{AEF} content was analyzed by Western blotting.

In vitro kinase assay. The in vitro kinase assay was performed essentially as previously described (39). For HeLa cells, subconfluent cultures in 60-mm-diameter dishes were treated with or without EGF (10 nM) for 15 min. The cells were then washed once with ice-cold PBS and scraped into 200 μl of lysis buffer (20 mM Tris-HCl [pH 7.5], 5 mM EGTA, 25 mM β-glycerophosphate, 1% Triton X-100, 2 mM dithiothreitol [DTT], 1 mM vanadate, 1 mM phenylmethylsulfonyl fluoride, aprotinin at 2 μg/ml). Cell debris was eliminated by centrifugation at $14,000 \times g$ for 20 min at 4°C. The supernatant was incubated with 45 μl of a 1:10 slurry of protein A-Sepharose–CL4B Sepharose beads, 10 μl (200 μg/ml) of goat anti-Erk5 antibody C-20, and 1 μl (2.5 μg/μl) of a rabbit anti-goat immunoglobulin G (Sigma) for 2 h at 4°C. The immunoprecipitates were washed twice with 20 mM Tris-HCl (pH 7.5)–500 mM NaCl–2 mM DTT–0.05% Tween 20, and then the precipitates were divided into two parts. The one used for the kinase assay was washed once with a buffer containing 20 mM Tris-HCl (pH 7.5), 2 mM EGTA, 2 mM DTT, and 1 mM phenylmethylsulfonyl fluoride and then incubated for 30 min at 30°C in 15 μl of a buffer containing 20 mM Tris-HCl (pH 7.5), 10 mM $MgCl_2$, 100 μM ATP, 10 μg of myelin basic protein (MBP), and 2 μCi of [γ-^{32}P]ATP. Kinase assays using GST-MEF2C were performed by replacing MBP in the kinase reaction with 5 μg of GST-MEF2C. The reactions were quenched by addition of an equal volume of 2× Laemmli sample buffer and subjected to SDS–10% PAGE. The gels were then exposed to a Fuji IIIS sensitive screen, and the radioactivity in the gels was digitally analyzed with a BAS1500 apparatus. Dried gels were also exposed to X-ray films to obtain autoradiographs.

Immunofluorescence microscopy. Cells plated on glass coverslips were washed with PBS and fixed in 2% *p*-formaldehyde for 30 min at room temperature. Monolayers were washed twice for 10 min each time with PBS supplemented with 0.1% (final concentration) Triton X-100 and then blocked in PBS with 1% BSA for 1 h at room temperature. Monolayers were then incubated with the primary antibody in blocking solution for 2 h at room temperature or overnight at 4°C. After three washes for 10 min each in PBS with 0.2% BSA, the coverslips were incubated with cyanine-3-conjugated secondary antibodies for 30 min, washed three times for 5 min each time in PBS with 0.2% BSA, and mounted. Samples were analyzed by regular epifluorescence microscopy or by confocal immunofluorescence microscopy using a Zeiss LSM 510 confocal microscope.

RESULTS

A phospho-Erk5 antibody that recognizes dually phosphorylated Erk5. To investigate whether the Erk5 pathway participates in NRG signal transduction, we first generated reagents that would allow an initial estimation of the action of ErbB receptors on the activation state of Erk5. The activation of Erk5 can be monitored by in vitro phosphorylation of sub-

Downloaded from http://mcb.asm.org/ on October 23, 2019 by guest

strates such as MBP (1), transcription factor MEF2C (40, 74), or Erk5 itself (2), as well as by a shift in the mobility of Erk5 (41). Antibodies were raised against peptides corresponding to the C terminus of Erk5 (residues 791 to 805) and to a phosphorylated peptide of the Erk5 activation loop (residues 213 to 225) (Fig. 1A). The latter includes the MAPK consensus microdomain TEY, whose dual phosphorylation is associated with stimulation of kinase activity (56). For the characterization of these reagents, we used HeLa cells whose treatment with EGF has been reported to trigger Erk5 activation (41). In agreement with such studies, stimulation of HeLa cells with EGF caused a retardation in the migration of Erk5, as indicated by immunoprecipitation and Western analysis with the antibody raised to the C terminus of Erk5 (Fig. 1B). Both Erk5 bands were absent when the immunoprecipitates were carried out with an excess of the peptide used for the immunization (data not shown). In vitro kinase studies showed that EGF significantly increased the phosphorylation of the exogenous substrates MBP and MEF2C by Erk5 (Fig. 1C). In addition, phosphorylation of endogenous Erk5 was also substantially increased in cells treated with the growth factor (Fig. 1C).

In HeLa cells treated with EGF, the anti-phospho-Erk5 antibody (anti-pErk5) immunoprecipitated the slower-migrating Erk5 band but failed to recognize the faster-migrating Erk5 form (Fig. 1D, top). In addition, when anti-Erk5 C-terminal immunoprecipitates were subjected to Western analysis with the anti-pErk5 antibody, a prominent band corresponding to the upper migrating Erk5 form was detected in cells treated with EGF (Fig. 1D, bottom). In these assays, two faster-migrating forms could also be detected, but only in EGF-treated samples (Fig. 1D; bottom, arrows). Transfection of HeLa cells with an HA-tagged version of a double Erk5 mutant in which the original TEY sequence required for activation was replaced with AEF (HA-Erk5^{AEF}) indicated that recognition of Erk5 by the anti-pErk5 serum required the phosphorylation at the TEY microdomain (Fig. 1E). In addition, the data obtained with this mutant indicated that the integrity of the TEY microdomain was essential for growth factor-induced changes in electrophoretic mobility, thus excluding the possibility that these changes were due to the phosphorylation of Erk5 that occurs at sites outside the activation domain (20). Dose-response curves of the effect of EGF on Erk5 activity in HeLa cells showed a correlation among Erk5 shifting, anti-pErk5 blots, and in vitro kinase activity (data not shown).

NRG receptors activate the Erk5 pathway. With the help of the above-described reagents, we tested whether the Erk5 pathway is involved in NRG signal transduction. The breast cancer cell line MCF7 contains NRG receptors and has been extensively used as a model with which to analyze NRG-induced responses (34, 51). First, the action of EGF and NRG on ErbB receptor activation was evaluated. Addition of NRG stimulated tyrosine phosphorylation of ErbB2, ErbB3, and ErbB4 in MCF7 cells (Fig. 2A). However, and due to the low complement of EGFR present in these cells, EGF and NRG failed to induce a significant increase in the tyrosine phosphorylation of the EGFR. In HeLa cells, EGF treatment stimulated tyrosine phosphorylation of the EGFR and ErbB2. EGF and NRG failed to induce ErbB3 or ErbB4 tyrosine phosphorylation.

In MCF7 cells, treatment with NRG resulted in activation of Erk5, as demonstrated by the gel retardation of Erk5 (Fig. 2A and B), by the selective recognition of the upper band by the anti-pErk5 antibody (Fig. 2B), by in vitro kinase assays using GST-MEF2C as an exogenous substrate (Fig. 2C), and by the autophosphorylation of Erk5 (Fig. 2D). To investigate if NRG affects the subcellular distribution of Erk5, the location of Erk5 was analyzed by immunofluorescence microscopy with the anti-Erk5 C terminus antibody (Fig. 2E). Under resting conditions, Erk5 was diffusely distributed in the cytosol and also appeared in the nucleus. NRG induced a substantial decrease in the cytosolic staining that was accompanied by accumulation in the nucleus (Fig. 2E; see also Fig. 5F).

The effect of NRG on Erk5 activation was found to be time and dose dependent. The maximal effect occurred at concentrations between 5 and 10 nM, and a half-maximal effect was obtained at 2 nM (Fig. 2F, top, and data not shown). The effect of NRG on Erk5 activation was detectable at 5 min of treatment, reached a maximum by 10 to 20 min, and decreased progressively to resting levels by 2 h (Fig. 2F, bottom).

Effect of signaling inhibitors on NRG-induced Erk5 activation. To analyze if NRG-dependent activation of Erk5 requires the kinase activity of the NRG receptors, MCF7 cells were preincubated with increasing concentrations of the ErbB receptor tyrosine kinase inhibitor DAPH (10) for 30 min before NRG addition. Treatment with this drug decreased ErbB2 tyrosine phosphorylation (Fig. 3A, top) and Erk5 activation (Fig. 3A, middle) in a dose-dependent fashion, suggesting that the kinase activity of NRG receptors is essential for NRG-induced Erk5 activation. The action of this drug on Erk5 mobility shift was more pronounced than its effect on p185^{ErbB2} tyrosine phosphorylation (Fig. 3A, bottom). However, DAPH was unable to prevent Erk5 activation in response to osmotic stress induced by sorbitol (Fig. 3B), indicating that DAPH did not affect other Erk5 activation routes.

Because of the high homology between structural domains of Erk1/2 and Erk5 (43, 76), the action of inhibitory treatments that target the Erk1/2 pathway was tested for its potential effect on Erk5 activation by NRG receptors. In several cell types, coupling of growth factor receptor tyrosine kinases to the Erk1/2 pathway has been reported to be mediated by the Ras/Raf pathway (42, 49). The participation of Ras in receptor-induced Erk5 activation has been less well defined. EGF-induced (41) or G protein-coupled receptor-induced (25) Erk5 activation has been reported to be independent of Ras activity, while NGF-induced Erk5 activation has been shown to be mediated by Ras (39) and the activity of Erk5 has been shown to be increased by Ras (20). The action of a dominant negative form of Ras (RasN17) on NRG-induced Erk5 activation was analyzed in MCF7 cells infected with retrovirus or in stable clones expressing different levels of RasN17. Overexpression of RasN17 in MCF7 cells failed to substantially affect NRG-induced activation of Erk5 (Fig. 3C). That this form acts as a bona fide Ras inhibitor in MCF7 cells was indicated by its ability to block NRG-induced Ras interaction with the Ras binding domain of Raf (data not shown). Furthermore, in parallel assays, RasN17 prevented the growth of NIH 3T3 fibroblasts (data not shown). Interestingly, RasN17 also failed to substantially affect NRG-induced Erk1/2 activation (Fig. 3C, bottom).

The action of U0126, an inhibitor of the Erk1/2 upstream

Downloaded from http://mcb.asm.org/ on October 23, 2019 by guest

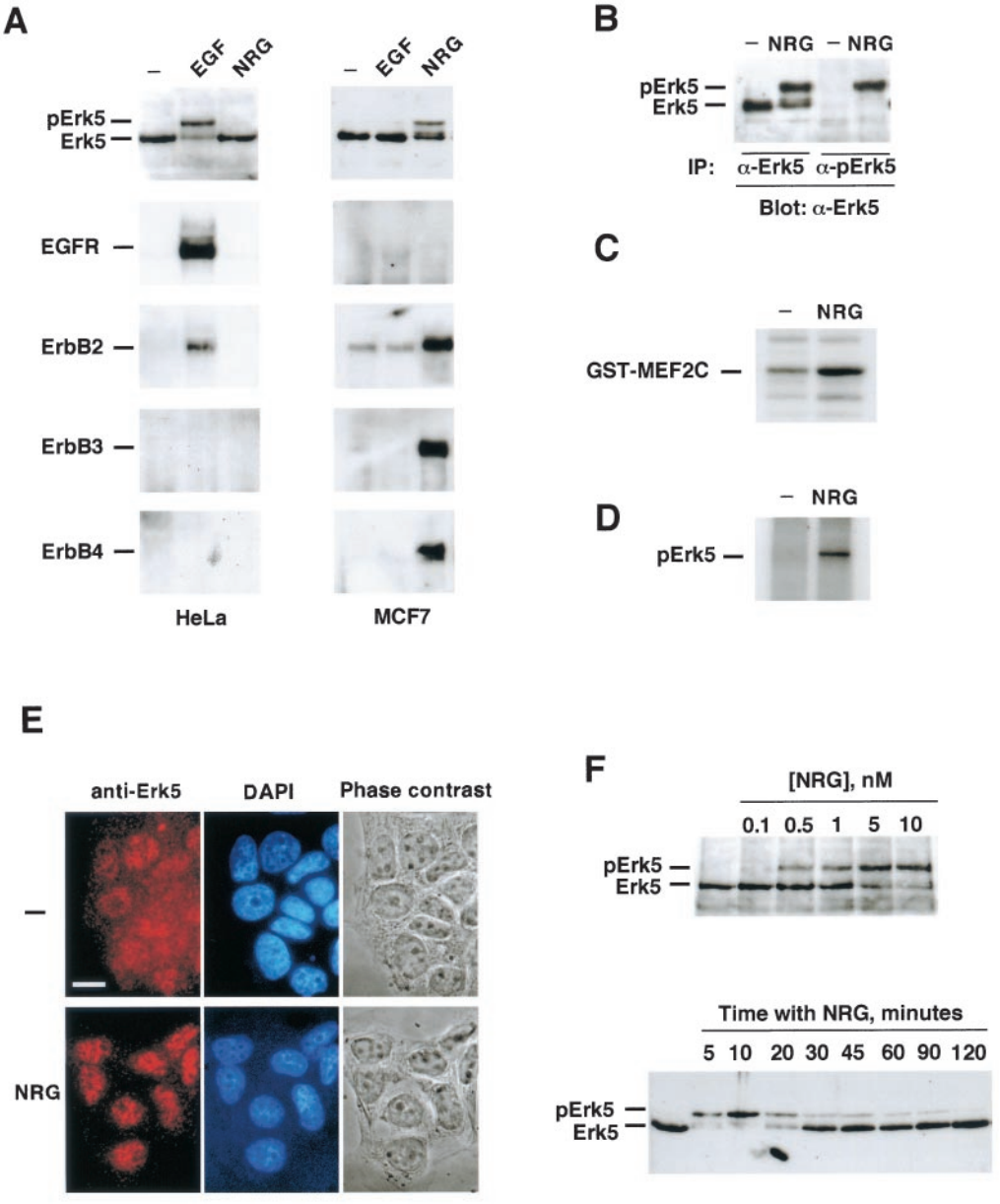

FIG. 2. Activation of Erk5 by NRG receptors. (A) HeLa (left) or MCF7 (right) cells were treated with EGF (10 nM) or NRG (10 nM) for 15 min. Lysates were analyzed by Western blotting with anti-Erk5 antibody C-20 (top) or immunoprecipitated (IP) with antibodies to EGFR, ErbB2, ErbB3, or ErbB4 and then subjected to SDS–6% PAGE. Blots of the immunoprecipitated receptors were probed with anti-phosphotyrosine antibodies. (B to D) Activation of Erk5, shown as specific identification of hyperactive Erk5 by the anti-pErk5 antibody (B) or by in vitro kinase studies using GST-MEF2C (C) or Erk5 autophosphorylation (D). In these experiments, 100-mm-diameter dishes of MCF7 cells were treated with 10 nM NRG for 15 min and lysates were prepared for immunoprecipitation. (E) Effect of NRG on the subcellular distribution of Erk5 in MCF7 cells. Where indicated, cells were treated with NRG for 30 min and then fixed. Immunofluorescence was carried out with the anti-Erk5 C terminus antibody, followed by Cy3-labeled anti-rabbit antibody. Bar, 20 μm. (F, top) Dose-response curve showing the effect of NRG on Erk5 activation. MCF7 cells were treated for 15 min with the indicated concentrations of NRG and then lysed, and 50 μg of the lysate was analyzed by Western blotting with the C-20 anti-Erk5 antibody. (F, bottom) Time course of NRG activation of Erk5. MCF7 cells were treated with 10 nM NRG for the indicated times. Lysates were processed by Western blotting as described above.

activating kinases (23), was also evaluated. Preincubation of MCF7 cells with this inhibitor resulted in a dose-dependent inhibition of NRG-induced Erk1/2 and Erk5 activation (Fig. 3D), with slightly higher potency toward Erk1/2.

Involvement of Erk5 in NRG-induced proliferation. Since NRG activated the Erk5 pathway and this MAPK pathway has been implicated in cell proliferation in response to EGFR activation (41), it was of interest to investigate the participation of this kinase in the growth responses to NRG. For this purpose, we expressed in MCF7 cells an HA-tagged form of Erk5 that has been reported to act in a dominant negative fashion (HA-Erk5^{AEF}; see reference 41). In MCF7 cells transfected with HA-Erk5^{AEF} (MCF7-Erk5^{AEF}), Western blot analysis with the anti-Erk5 antibody showed a retarded migration of

Downloaded from http://mcb.asm.org/ on October 23, 2019 by guest

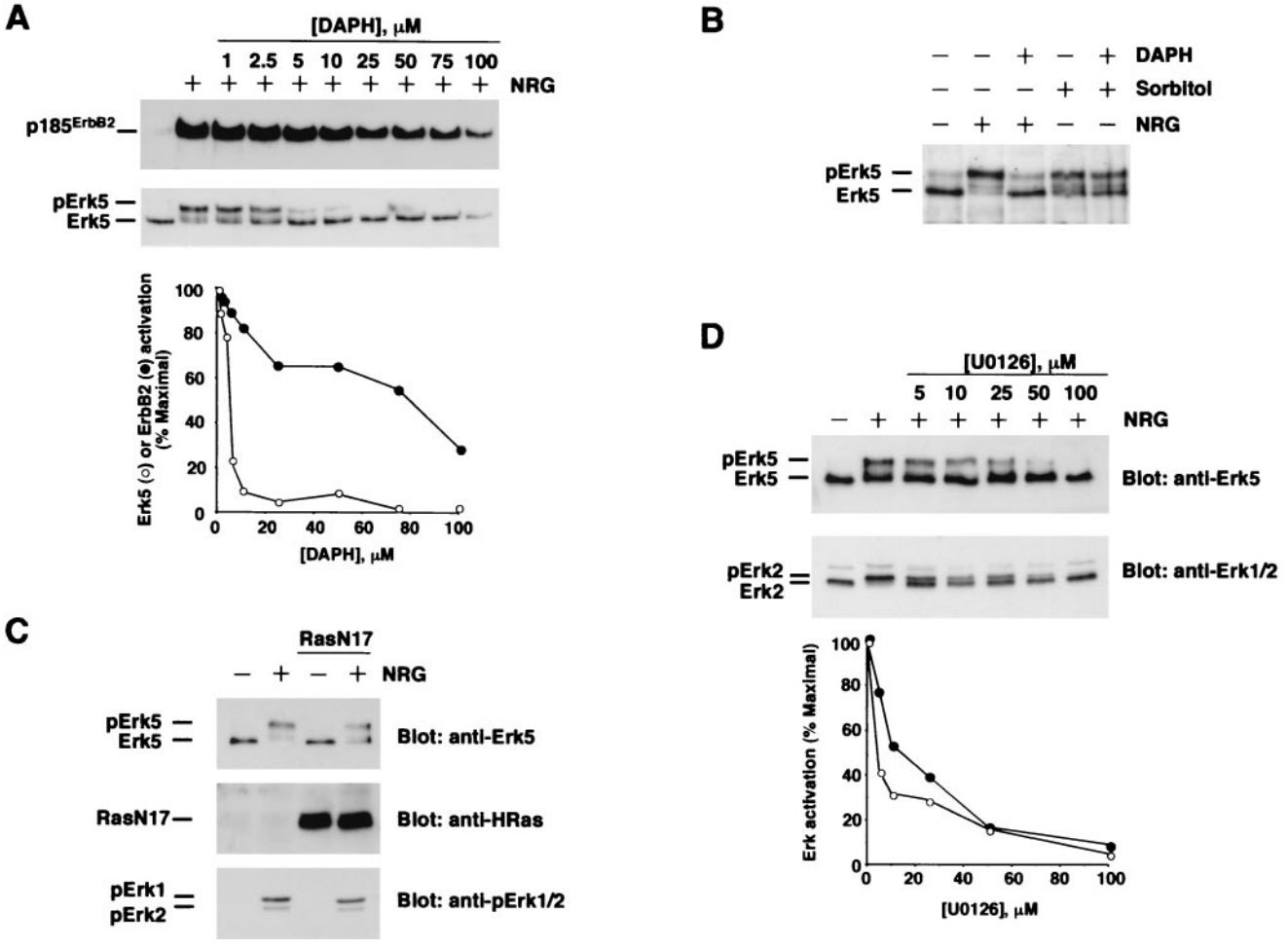

FIG. 3. Effects of several signaling inhibitors on NRG-induced Erk5 activation. (A) Dose effect of the tyrosine kinase inhibitor DAPH on NRG-induced Erk5 activation. MCF7 cells were preincubated with DAPH at the indicated concentrations for 30 min before NRG (10 nM) addition. Incubations were extended for an additional 15 min, and then samples were lysed and subjected to immunoprecipitation with the 4D5 anti-ErbB2 antibody (top) or 50 μg of the lysate was directly loaded onto an SDS–6% PAGE gel (bottom). The Western blots were probed with anti-phosphotyrosine (top) or anti-Erk5 C-20 (bottom) antibody. The bottom graphic is a representation of the data presented in the blot. (B) Effect of DAPH on sorbitol-induced Erk5 activation. The preincubations and treatments were as described for panel A, but sorbitol (0.4 M) was added to the indicated samples and they were incubated for 15 min. (C) Effect of RasN17 on Erk5 activation by NRG. MCF7 cells were infected with pLZR-RasN17-IRES-GFP or with empty-vector-containing retroviruses. At 48 h later, cells were treated with 10 nM NRG for 15 min and then lysed. A 15-μg sample of the lysate was analyzed for RasN17 content with an anti-HRas antibody (middle) or probed with the anti-pErk antibody (bottom), and the rest of the sample was immunoprecipitated with the anti-Erk5 C terminus antibody. Western blotting of Erk5 was performed with the C-20 anti-Erk5 antibody (top). (D) Effect of U0126 on NRG-induced Erk5 and Erk1/2 activation. MCF7 cells were preincubated with the indicated concentrations of U0126 for 30 min before the addition of 10 nM NRG. Cells were then lysed, and 10 μl was analyzed by SDS–10% PAGE and Western blotting with an anti-Erk1/2 antibody (bottom). The rest of the sample was immunoprecipitated with the anti-Erk5 C terminus antibody and loaded onto 6% polyacrylamide gels. The blot shown at the top was probed with the C-20 anti-Erk5 antibody. A quantitative representation of the data obtained in the blot is shown at the bottom. Erk5 (●) and Erk2 (○) activation was measured as the ratio between the slow- and faster-migrating forms of these kinases. Maximal activation was considered to be that obtained with NRG in the absence of U0126.

the HA-Erk5^{AEF} form with respect to endogenous Erk5, probably due to the presence of the HA tag at the N terminus (Fig. 4A, left). Western blotting with the anti-HA antibody demonstrated that the upper band in MCF7-Erk5^{AEF} cells corresponded to the transfected HA-Erk5^{AEF} dominant negative form (Fig. 4A, right).

To test the effect of HA-Erk5^{AEF} on NRG-induced cell proliferation, we used several strategies to express HA-Erk5^{AEF}. Expression of HA-Erk5^{AEF} by retrovirus infection (Fig. 4B) resulted in a significant decrease in NRG-induced MCF7 cell proliferation, compared to the effect of NRG on cells infected with the empty vector (Fig. 4B). This effect was maximal within 4 to 7 days of NRG treatment. Analogous data were obtained when a clone of MCF7 cells was used in which the expression of HA-Erk5^{AEF} was under the control of the tetracycline transactivator (MCF7-Erk5^{AEF}-Tet-Off cells, Fig. 4C). Finally, studies of the proliferation of MCF7 clones constitutively expressing different levels of HA-Erk5^{AEF} indicated a negative correlation between the level of HA-Erk5^{AEF} and the degree of NRG-induced cell proliferation (Fig. 5E and data not shown).

To gain insight into the mechanism by which HA-Erk5^{AEF}

Downloaded from http://mcb.asm.org/ on October 23, 2019 by guest

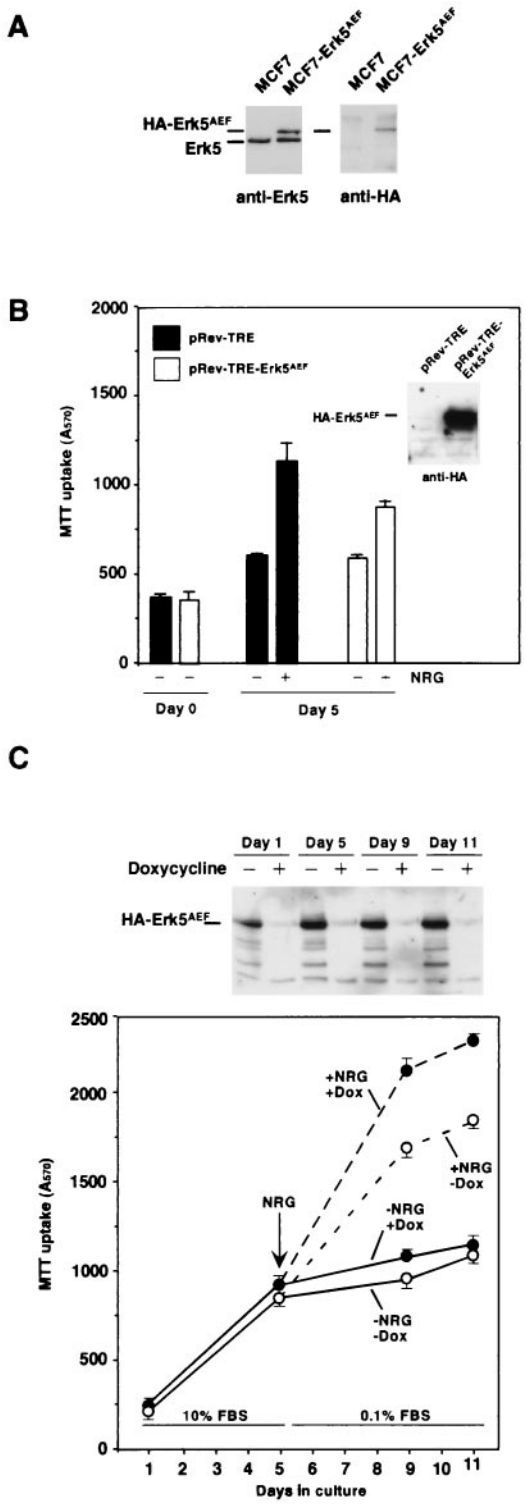

FIG. 4. Expression of a dominant negative form of Erk5 inhibits NRG-induced MCF7 proliferation. (A) Expression of HA-tagged Erk5^{AEF} in MCF7 cells. Expression of the mutant protein (HA-Erk5^{AEF}) in MCF7 cells transfected with pCEFL-HA-Erk5^{AEF}. Western blots were probed with anti-Erk5 (left) or anti-HA (right) antibody. (B) Effect of NRG on the proliferation of wild-type MCF7 and MCF7-Erk5^{AEF} cells. MCF7 cells were infected with pRev-TRE-HA-Erk5^{AEF} or with empty-vector-containing retrovirus (pRev-TRE), and cell proliferation was measured in the presence or absence of NRG (10 nM) as described in Materials and Methods. The results are the mean ± SD of quadruplicate measurements of an experiment that was repeated at least three times. Closed bars represent the A_{570} of MCF7 cells infected with pRev-TRE, and open bars correspond to the A_{570} of MCF7 cells infected with pRev-HA-Erk5^{AEF}. (C) Proliferation of MCF7-HA-Erk5^{AEF}-Tet-Off in response to NRG. MCF7-HA-Erk5^{AEF}-Tet-Off cells were plated in the absence (white-filled circles) or presence (black-filled circles) of doxycycline at 10 ng/ml and cultured for up to 5 days in the presence of 10% serum. At day 5, cells were switched to 0.1% FBS and treated with 10 nM NRG and the cultures were maintained with or without doxycycline, as indicated. Cell proliferation was measured by the MTT assay at the indicated points. The regulated expression of HA-Erk5^{AEF} in MCF7-HA-Erk5^{AEF}-Tet-Off cells was analyzed by Western blotting with the anti-HA antibody (top).

affects NRG signal transduction in MCF7 cells, we evaluated how HA-Erk5^{AEF} affects (i) upstream signals triggered by ErbB receptor activation; (ii) the activation of endogenous Erk5; (iii) the subcellular location of Erk5; and (iv) downstream signaling pathways, such as c-*jun* induction (40, 45), that depend on Erk5 activation. For these studies, we used MCF7 cells expressing undetectable, intermediate (MCF7-Erk5^{AEF} clone 17, expressing HA-Erk5^{AEF} in an approximate ratio of 1:1 with respect to endogenous Erk5), and high levels of HA-Erk5^{AEF} (MCF7-Erk5^{AEF} clone 11).

Expression of HA-Erk5^{AEF} did not affect the levels of ErbB2 (Fig. 5A) or the response to NRG in terms of early signaling events, such as ErbB2 (Fig. 5A) or Shc (Fig. 5B) tyrosine phosphorylation, or association of the receptor with the adaptor molecule (Fig. 5B, bottom). In MCF7-Erk5^{AEF} clone 17 cells, NRG was able to stimulate an endogenous Erk5 mobility shift (Fig. 5C) and Erk5 phosphorylation in in vitro kinase assays (Fig. 5D). This effect of NRG mobility shift on endogenous Erk5 was also found in two other clones expressing intermediate levels of HA-Erk5^{AEF} (data not shown). However, in cells expressing high levels of HA-Erk5^{AEF}, NRG treatment failed to induce an endogenous Erk5 mobility shift (Fig. 5C).

Even though NRG efficiently stimulated an Erk5 mobility shift in MCF7-HA-Erk5^{AEF} clone 17 cells, these cells (and another clone with a similar HA-Erk5^{AEF}/endogenous Erk5 ratio) proliferated less than wild-type MCF7 cells. On the other hand, the proliferation of MCF7-HA-Erk5^{AEF} clones expressing intermediate levels of HA-Erk5^{AEF} was greater than that of the clones expressing high levels of HA-Erk5^{AEF} (Fig. 5E and data not shown).

The above data indicated that HA-Erk5^{AEF} could act on cell proliferation by mechanisms other than interference with endogenous Erk5 phosphorylation. An important step in the regulation of cell proliferation by MAPKs is their transport to the nucleus upon activation (9). To investigate whether expression HA-Erk5^{AEF} affects NRG-induced Erk5 translocation, the cellular distribution of Erk5 was analyzed by immunofluorescence using the affinity-purified anti-Erk5 C terminus antibody. As shown above, in MCF7 cells, NRG induced the translocation and accumulation of Erk5 in the nuclear compartment (Fig. 5F and 2E). In clone 17, NRG-induced Erk5 translocation to the nucleus was profoundly inhibited, as indicated by quantitative analysis of the subcellular distribution of Erk5 (Fig. 5F, right).

Finally, the possibility that the Erk5 pathway could mediate

Downloaded from http://mcb.asm.org/ on October 23, 2019 by guest

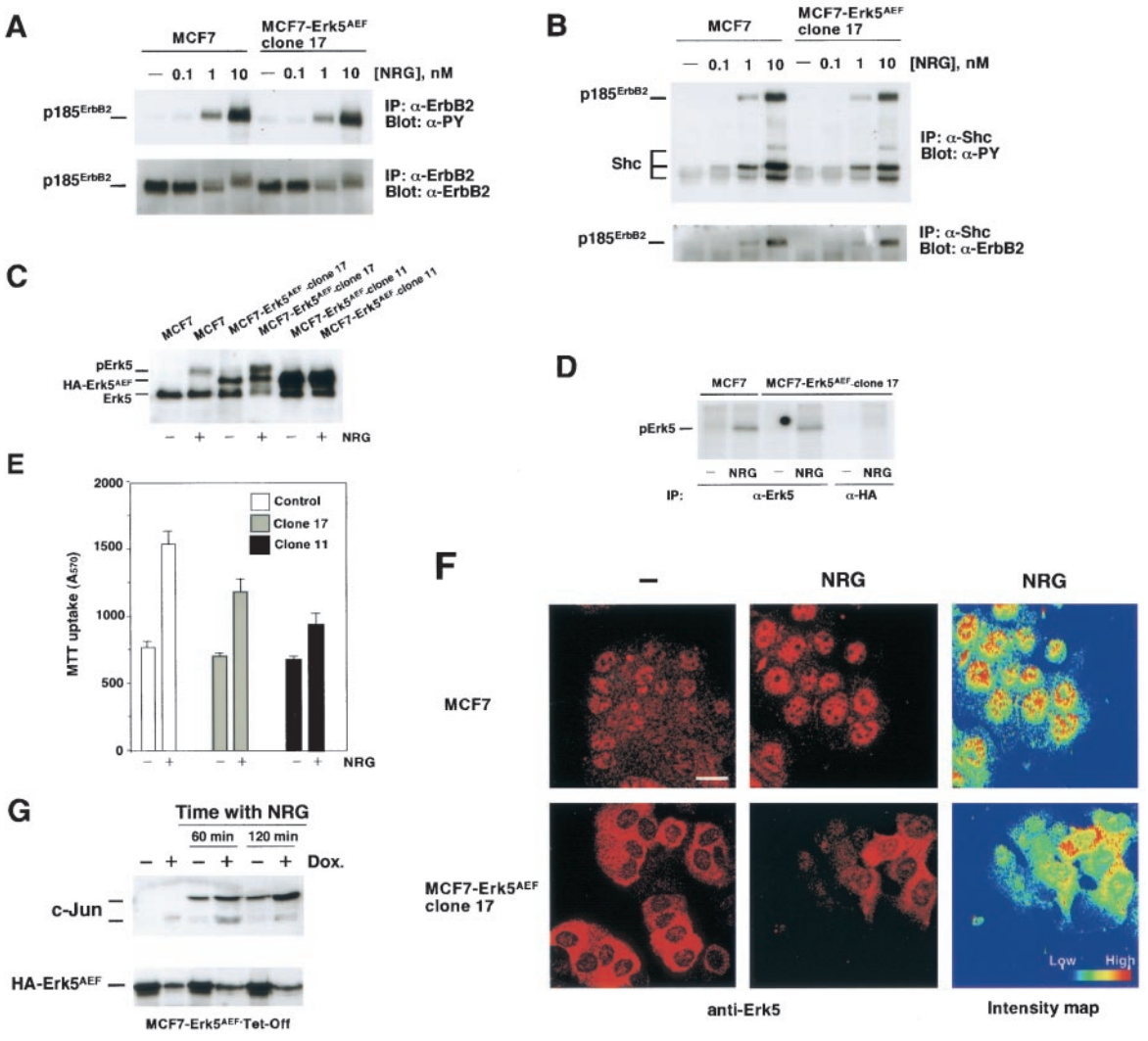

FIG. 5. The Erk5^{AEF} form affects nuclear translocation of Erk5. (A) Activation of ErbB2 by NRG in MCF7 and MCF7-Erk5^{AEF} cells. MCF7 and MCF7-Erk5^{AEF} cells were incubated in the presence of increasing concentrations of NRG for 15 min. Cells were then lysed and immunoprecipitated (IP) with anti-ErbB2 antibody 4D5. The Western blot shown was probed with anti-phosphotyrosine (α-PY) antibody (top), stripped, and reprobed with the Ab-3 anti-ErbB2 antibody (bottom). (B) Tyrosine phosphorylation of Shc and association to ErbB2. MCF7 and MCF7-Erk5^{AEF} cells plated and treated as described above were lysed and immunoprecipitated with an anti-Shc antibody. The blot was probed with anti-phosphotyrosine antibody (top), stripped, and then reprobed with the Ab-3 anti-ErbB2 antibody (bottom). (C) Wild-type MCF7, a clone of MCF7-Erk5^{AEF} cells expressing intermediate levels of HA-Erk5^{AEF} (clone 17), and a clone of MCF7-Erk5^{AEF} cells expressing high levels of HA-Erk5^{AEF} (clone 11) were treated with NRG for 15 min, and then lysates were prepared for immunoprecipitation with the anti-Erk5 C terminus antibody. The blot was then probed with the C-20 antibody. (D) In vitro autophosphorylation of Erk5 in wild-type MCF7 and MCF7-Erk5^{AEF} clone 17 cells. Cells were treated with NRG (10 nM) for 15 min and then equal amounts of cell extract were immunoprecipitated with the anti-Erk5 C terminus antibody (both cell lines) or the anti-HA antibody (MCF7-Erk5^{AEF} clone 17 cells). In vitro kinase assays were then performed as described above. (E) Proliferation of MCF7, MCF7-Erk5^{AEF} clone 17, and MCF7-Erk5^{AEF} clone 11 cells. Plating, treatment with 10 nM NRG, and measurement of cell proliferation were done as described in Materials and Methods. (F) Effect of HA-Erk5^{AEF} on the nuclear translocation of Erk5. Wild-type or clone 17 MCF7 cells were plated on coverslips and stimulated for 60 min with NRG (10 nM, center). Immunofluorescent staining was done with the anti-Erk5 C terminus antibody. Images were taken with a confocal microscope with identical settings. Quantitation of the intensity in each pixel of the central images is shown at the right (intensity map). Bar, 20 μm. (G) NRG-induced c-Jun up-regulation in MCF7-Erk5^{AEF}-Tet-Off cells. Cells were cultured in the absence or presence of doxycycline (Dox.; 10 ng/ml) and treated with 10 nM NRG for the indicated times. Protein concentrations were measured, equal amounts of the cell lysates were subjected to SDS–10% PAGE, and Western blots were probed with an anti-c-Jun antibody (top) or an anti-HA antibody (for HA-Erk5^{AEF}; bottom).

the effect of NRG on c-Jun levels was analyzed. The levels of c-Jun were analyzed by Western blotting in MCF7-HA-Erk5^{AEF}-Tet-Off cells. In cells cultured with doxycycline, NRG substantially increased c-Jun levels (Fig. 5G). This effect was detectable within 15 to 30 min, reached a maximum at 120 min, and decreased thereafter (Fig. 5G and data not shown). An increase in the amount of HA-Erk5^{AEF} caused by withdrawal of doxycycline had a significant inhibitory effect on NRG-induced c-Jun up-regulation.

Constitutive activation of Erk5 in breast cancer cell lines. Since several human solid tumors express constitutively active forms of ErbB receptors, the activation status of Erk5 was

Downloaded from http://mcb.asm.org/ on October 23, 2019 by guest

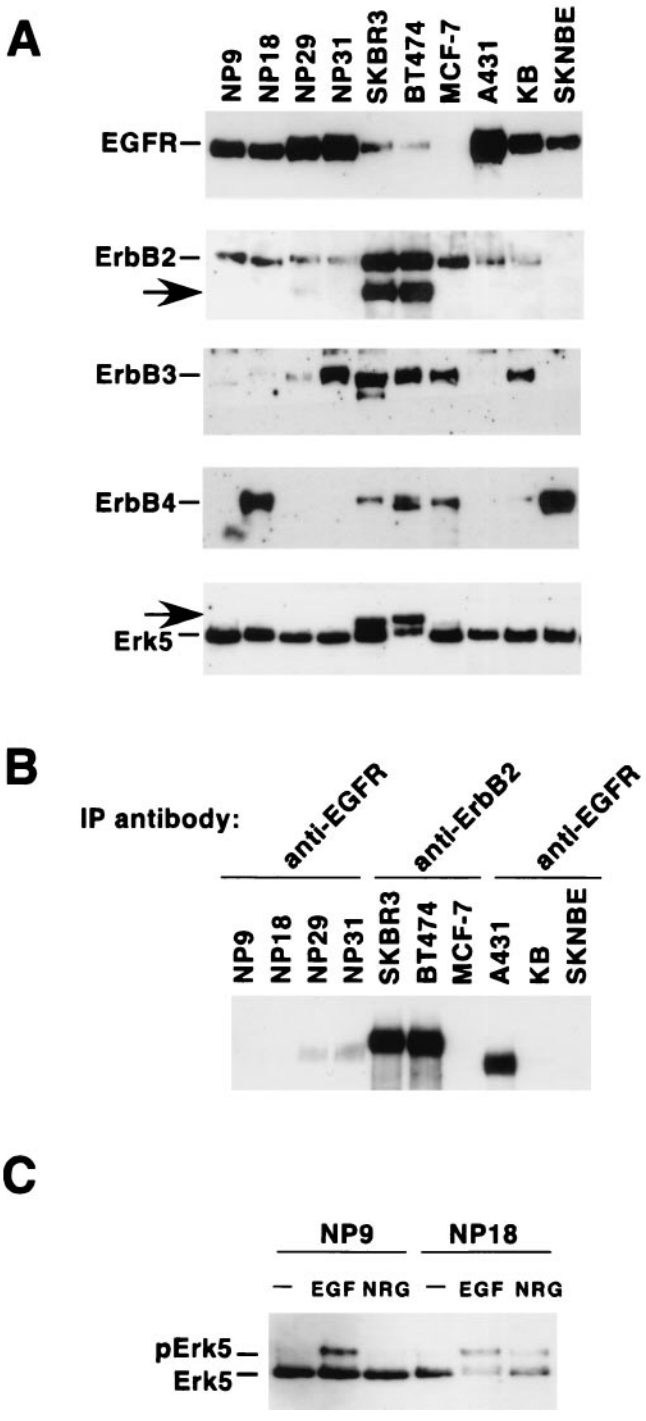

FIG. 6. Expression of ErbB receptors and Erk5 in human cancer tumor cell lines. (A) Exponentially growing cultures of each of the cell lines shown were lysed, and 1 mg of cell lysate was immunoprecipitated (IP) with the respective anti-ErbB antibody (528 for the EGFR, 4D5 for ErbB2, C-17 for ErbB3, and C-18 for ErbB4). The immunoprecipitates were then subjected to SDS–6% PAGE, and after electrophoresis, the proteins were transferred to polyvinylidene difluoride membranes. Blots were probed with the R03 rabbit polyclonal antibody (EGFR), Ab-3 (ErbB2), C-17 (ErbB3), and C-18 (ErbB4). The arrow in the ErbB2 blot corresponds to a truncated version of the ErbB2 receptor. In parallel, 1 mg of protein lysate was immunoprecipitated with the anti-Erk5 C terminus antibody and the Western blot was probed with the C-20 anti-Erk5 antibody (bottom). The arrow in the Erk5 blot indicates a form of Erk5 with decreased electrophoretic mobility. (B) Resting level of tyrosine phosphorylation of ErbB receptors in the cells shown in panel A. One milligram of protein from cell lysates was immunoprecipitated with the indicated anti-ErbB antibodies, and the Western blot was probed with anti-phosphotyrosine antibodies. (C) Effects of NRG and EGF on Erk5 activation in pancreatic cell lines overexpressing EGFR. NP cell lines were treated for 15 min with EGF (10 nM) or NRG (10 nM). Lysates were then immunoprecipitated with the anti-Erk5 C terminus antibody, and the blots were probed with the C-20 anti-Erk5 antibody.

analyzed in a panel of tumoral cell lines expressing different combinations of ErbB receptors (Fig. 6A). In breast cancer cell lines SKBR3 and BT474, in addition to the fast-migrating form of Erk5, a slower-migrating form was also present (Fig. 6A, arrow at the bottom). Analyses of the ErbB receptor content of these cell lines indicated that ErbB2 and a truncated form of this receptor that migrates faster than the holoreceptor (22) were the mainly overexpressed ErbB receptors in SKBR3 and BT474 cells (Fig. 6A). Interestingly, in the cell lines overexpressing the EGFR, such as epidermoid cell-derived A431 and KB and the pancreatic carcinoma NP9, NP18, NP29, and NP31 cell lines, the mainly detectable form of Erk5 corresponded to the faster-migrating form, even though the EGFR was tyrosine phosphorylated under resting conditions, especially in A431 cells (Fig. 6B). These cell lines, however, maintained responsiveness of the Erk5 pathway to EGF (Fig. 6C and data not shown).

Attempts to investigate the nature of the retarded forms of Erk5 in the BT474 and SKBR3 cell lines were carried out. We considered three possibilities: (i) continuous upstream stimulation of Erk5 by constitutively active receptors, (ii) a molecularly aberrant form of Erk5 that would result in anomalous mobility, and (iii) a defect in the dephosphorylation of Erk5. An estimation of the latter possibility was performed by analysis of the overall phosphatase activity of BT474 and SKBR3, together with reverse transcription-PCR studies of the expression of the phosphatases MKP3 and CL100, which have been implicated in Erk5 dephosphorylation (39). In BT474 and SKBR3 cells, enzymatic assays of phosphatase activity indicated that these cells do not have any gross defect in phosphatase activity compared to cell lines, such as MCF7, that efficiently dephosphorylate Erk5 (data not shown). In addition, in BT474 cells, reverse transcription-PCR analyses of CL100 and MKP3 indicated that this cell line expresses both phosphatases (data not shown). While other, undefined phosphatases may also act to dephosphorylate Erk5, these data suggested that no major defects in phosphatase activity could explain the higher-M_r form of Erk5 present in BT474 and SKBR3 cells.

A strong indication that the upper form of Erk5 present in BT474 and SKBR3 cells could correspond to a constitutively hyperactive form was supported by its identical mobility in SDS-PAGE gels compared to the NRG-induced shift in Erk5 (Fig. 7A). Use of the anti-pErk5 antibody demonstrated that, in fact, the retarded form corresponded to a dually phosphorylated form of Erk5 (Fig. 7A, right). The intensity of this band, present under nonstimulating conditions, increased upon NRG treatment. NRG induced an almost complete shift of the faster-migrating form into the form with retarded migration. Immunofluorescent staining with the anti-Erk5 C terminus an-

Downloaded from http://mcb.asm.org/ on October 23, 2019 by guest

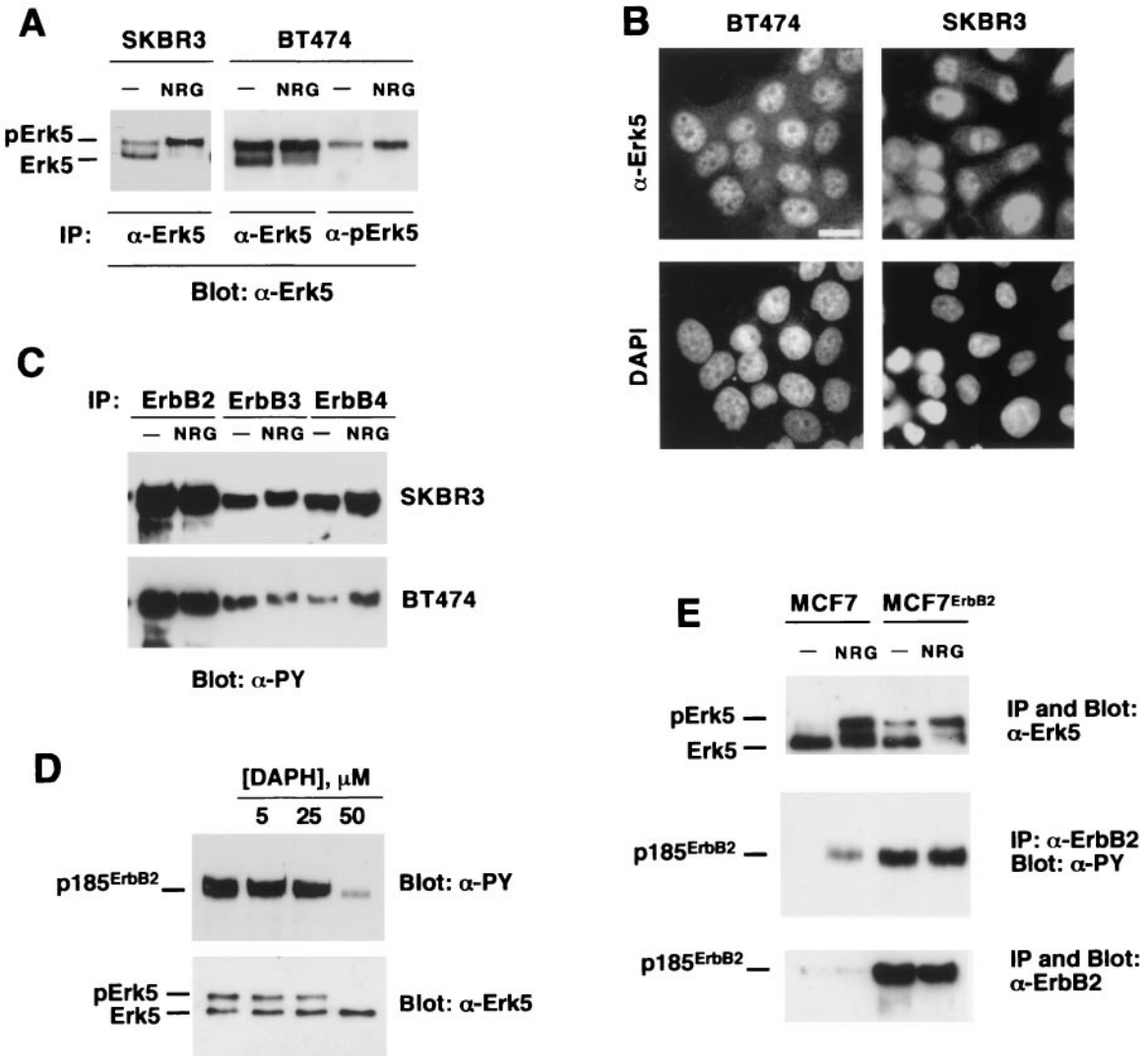

FIG. 7. Mechanism of generation of the retarded Erk5 form in breast cancer cells. (A) The upper Erk5 band present in BT474 cells is recognized by the anti-pErk5 antibody. SKBR3 or BT474 cells were treated with NRG (10 nM) for 15 min, and then lysates were immunoprecipitated (IP) with the anti-Erk5 C terminus or the anti-pErk5 antibody. Blots were then probed with the anti-Erk5 C-20 antibody. The blots show that the upper Erk5 band actually comigrates with the NRG-induced slow-migrating Erk5 form. (B) Immunofluorescent detection of Erk5 in BT474 and SKBR3 cells. Cells were stained with the anti-Erk5 antibody and counterstained with DAPI to show the nuclei. Bar, 20 μm. (C) Resting activation of NRG receptors in SKBR3 and BT474 cells. Where indicated, cells were treated with NRG (10 nM, 15 min), lysed, and immunoprecipitated with specific anti-ErbB receptor antibodies. Blots were probed with anti-phosphotyrosine (α-PY) antibodies. (D) Effect of DAPH on tyrosine-phosphorylated $p185^{ErbB2}$ and pErk5 levels. BT474 cells were treated overnight with the indicated concentrations of DAPH, and then lysates were immunoprecipitated with the 4D5 anti-ErbB2 antibody or with the anti-Erk5 C terminus antibody. The blots were probed with anti-phosphotyrosine (anti-ErbB2 immunoprecipitates) or anti-Erk5 C-20 (anti-Erk5 immunoprecipitates) antibody. (E) MCF7 cells and a clone overexpressing ErbB2 (MCF7-ErbB2) were treated, as indicated, with NRG (10 nM) and lysed, and 1 mg of cell protein was immunoprecipitated with anti-Erk5 C terminus antibody (top) or the 4D5 anti-ErbB2 antibody. The Western blot at the top was probed with anti-Erk5 C-20 antibody. The Western blot at the middle was probed with anti-phosphotyrosine antibodies that were then stripped. The blot was then reprobed with the Ab-3 anti-ErbB2 antibody (bottom).

tibody indicated that Erk5 was located predominantly in the nuclei of BT474 and SKBR3 cells (Fig. 7B). This staining was specific, since preincubation of the anti-Erk5 C terminus antibody with the peptide against which the antiserum was raised prevented nuclear staining (data not shown). In contrast to BT474 and SKBR3 cells, Erk5 was predominantly cytosolic in NP9 cells.

The above data suggested that the retarded band probably corresponded to constitutively active Erk5 rather than a molecularly aberrant Erk5 form and, together with the phosphatase data, indicated that the constitutive activation state of Erk5 could be due to continuous positive signaling upstream of Erk5. This latter hypothesis was then tested. Western blotting with anti-phosphotyrosine antibodies of anti-ErbB2, anti-ErbB3, and anti-ErbB4 immunoprecipitates from SKBR3 and BT474 cells indicated that these receptors were highly tyrosine phosphorylated under resting conditions (Fig. 7C), especially in the case of the overexpressed ErbB2 receptor. Because of

Downloaded from http://mcb.asm.org/ on October 23, 2019 by guest

the high phosphotyrosine content of these receptors under resting conditions, it was difficult to detect a clear stimulation of their tyrosine phosphorylation upon NRG treatment. A small shift in the electrophoretic mobility of ErbB3 in the NRG-treated samples from SKBR3 cells was an indirect indication of receptor activation (Fig. 7C). In cells treated with DAPH, this tyrosine kinase inhibitor decreased the amount of tyrosine-phosphorylated ErbB2 and also caused a change in the pattern of Erk5 forms toward the faster-migrating form (Fig. 7D).

To further investigate whether constitutively active ErbB receptors could continuously stimulate the Erk5 pathway, MCF7 cells were transfected with the human ErbB2 cDNA in order to increase the autocthonous content of ErbB2. ErbB2 overexpression in MCF7 cells resulted in constitutive activation of ErbB2 and Erk5 (Fig. 7E), the latter of which was shown by gel shifting to have a more retarded M_r. However, and probably because the MCF7-ErbB2 clones selected contained less ErbB2 than SKBR3 or BT474 cells, the amount of constitutively active Erk5 in MCF7-ErbB2 clones was significantly smaller than that present in SKBR3 or BT474 cells. In MCF7-ErbB2 cells, NRG was still able to activate Erk5 (Fig. 7E).

Participation of Erk5 in BT474 proliferation. Since Erk5 was important for the growth of MCF7 cells and because of the resting presence of activated Erk5 in BT474 cells, we investigated whether Erk5 also participates in BT474 proliferation. The effect of the HA-Erk5^{AEF} dominant negative form of Erk5 on the growth of BT474 cells was analyzed on BT474 cells infected with a retroviral bicistronic vector that coded for GFP and HA-Erk5^{AEF} (pLZR-HA-Erk5^{AEF}-IRES-GFP) or with an empty vector that only produced GFP (pLZR-IRES-GFP). In addition, the growth properties of two pools of BT474 cells expressing HA-Erk5^{AEF} were analyzed. Infection with pLZR-HA-Erk5^{AEF}-IRES-GFP resulted in expression of the dominant negative Erk5 form, as indicated by Western blotting with the anti-HA antibody (Fig. 8A). Even though there was resting stimulation of endogenous Erk5 in BT474 cells, transfected HA-Erk5^{AEF} electrophoretically migrated at a position that corresponded to the HA-Erk5^{AEF} of unstimulated MCF7-Erk5^{AEF} cells (Fig. 8B). In BT474, the dominant negative form was predominantly a cytosolic protein, as indicated by staining with the anti-HA antibody (Fig. 8C). This is in contrast to the clear nuclear location of Erk5 in untransfected BT474 cells (Fig. 7B and 8C). In BT474 cells expressing HA-Erk5^{AEF}, staining with the anti-Erk5 C terminus antibody showed that most of the nuclear Erk5 staining disappeared (Fig. 8C). Staining with an antibody that recognized Erk1 and Erk2 showed that these proteins were mainly cytosolic and that their subcellular distribution was unaffected by HA-Erk5^{AEF} expression (Fig. 8C).

Analyses of growth curves of cells infected with pLZR-HA-Erk5^{AEF}-IRES-GFP indicated that Erk5 participated in serum-induced proliferation of BT474 cells (Fig. 8D). At a low serum concentration (0.1%), both BT474 and BT474-Erk5^{AEF} proliferated at similar rates. In the presence of 1 or 10% serum, BT474 proliferated more than cells expressing the Erk5^{AEF} form. Analogous results were obtained when two different pools of BT474 cells that had been transfected with pCDNA3-HA-Erk5^{AEF} were used (data not shown). Taken together, these data suggest that Erk5 participates in BT474 cell growth.

DISCUSSION

Recent studies have indicated that the Erk5 pathway, besides transducing stress signals (1, 2), may also mediate proliferation in response to EGFR stimulation (41). Based on this finding and the importance of other ErbB receptors in breast cancer, we investigated if these other receptors could also activate the Erk5 pathway and whether that activation correlates with cell proliferation. Here we show that the Erk5 pathway is activated by NRG and that this MAPK pathway participates in proliferative responses induced by NRG receptors. We also provide evidence indicating that breast cancer cells that overexpress ErbB2 contain constitutively active Erk5 and that this kinase participates in their proliferation.

In breast cancer cell line MCF7, NRG activated Erk5, as indicated by NRG-induced in vitro phosphorylation of the Erk5 substrates MEF2C and MBP, autophosphorylation of Erk5, a shift of Erk5 to a slower-migrating form that corresponds to activated Erk5 (41), and detection of phosphorylated Erk5 by an antibody directed to a phosphopeptide that includes the consensus phosphorylation site TEY present in the activation loop of Erk5 (43) and other MAPKs (70). This antibody precipitated Erk5 and recognized the dually phosphorylated form of this kinase in Western blots. In addition, the antibody also precipitated activated forms of Erk1/2 (J. C. Montero and A. Pandiella, unpublished data). This was not surprising due to the high homology between Erk5 and Erk1/2 in the activating region (43). While this cross-reaction prevented its use as a specific reagent in immunofluorescence or in vitro kinase assays, the fact that Erk5 and Erk1/2 substantially differ in molecular mass (Erk5, 120 kDa; Erk1, 44 kDa; Erk2, 42 kDa) makes this reagent a valuable tool for studies of Erk5 activation by Western blot assay. Furthermore, the anti-pErk5 antibody may be used to detect constitutively active forms of Erk5, as shown here in BT474 breast cancer cells.

In contrast to the activation route of Erk1/2 (47, 70), little is known about the upstream signaling events that result in Erk5 activation. Genetic interaction studies have suggested that MEK5 acts as the major Erk5-activating kinase (76), with MEKK3 being an upstream activating kinase for MEK5 (14). How regulation of this kinase route is linked to ErbB receptor activation is not known. In our experimental system, NRG-induced Erk5 activation was sensitive to inhibitory drugs that preferentially act on receptor tyrosine kinases of the ErbB type. This conclusion was based on the data obtained with the ErbB-specific inhibitor DAPH (10). This drug has been shown to be a selective inhibitor of the EGFR and ErbB2 with respect to other receptor tyrosine kinases, such as the platelet-derived growth factor receptor, or even itinerant tyrosine kinases, such as Src family kinases. DAPH inhibited NRG-induced activation of Erk5 and ErbB2 in a dose-dependent fashion at concentrations known to specifically inhibit ErbB receptors. Therefore, as occurs with most other signaling events triggered by activation of ErbB receptors, including activation of Erk5 in HeLa cells (41), activation of Erk5 by NRG depends on the kinase activity of these receptors.

Studies on the participation of the Ras/Raf pathway in Erk5

Downloaded from http://mcb.asm.org/ on October 23, 2019 by guest

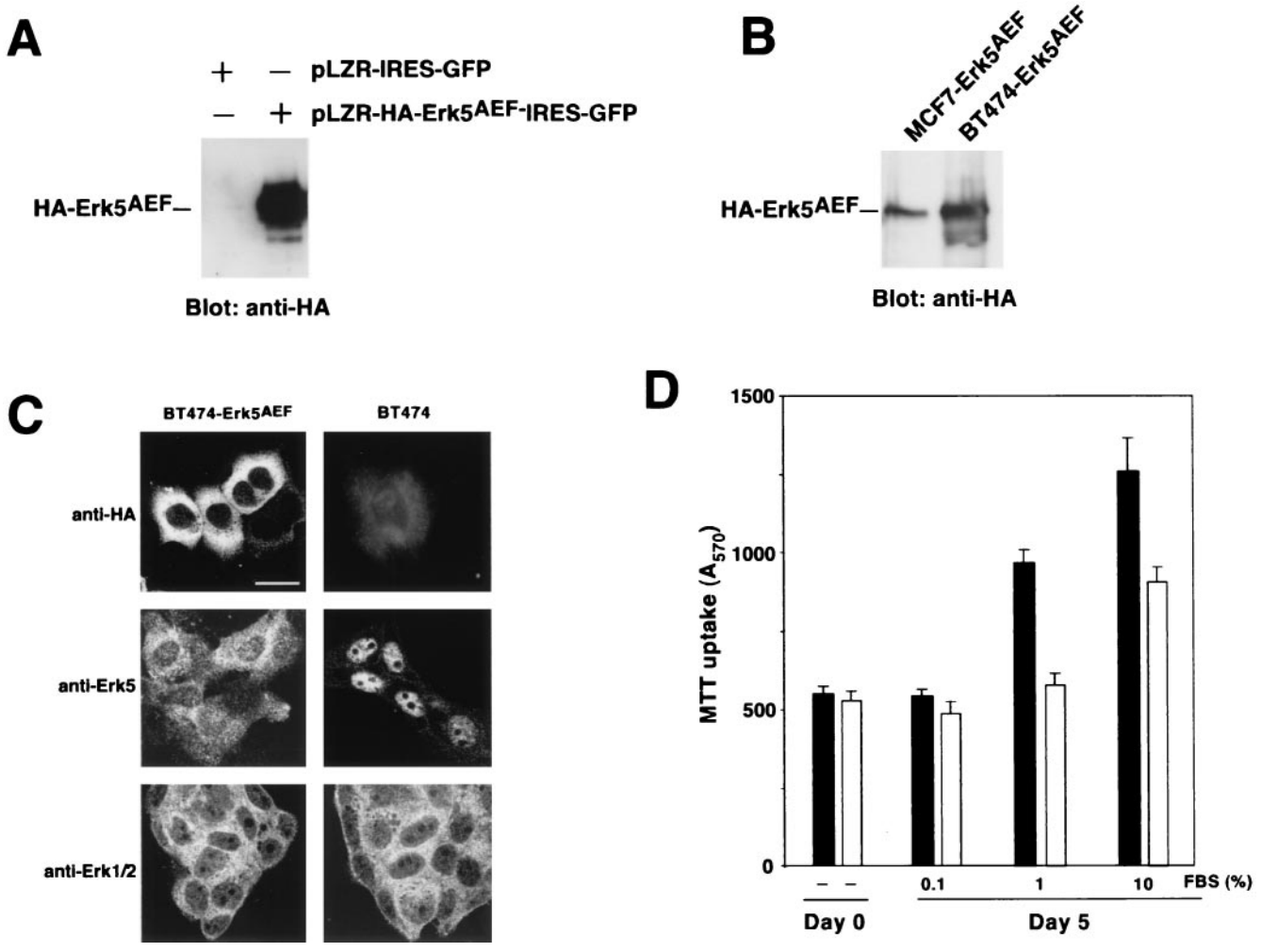

FIG. 8. Proliferation of BT474 cells expressing the HA-Erk5^{AEF} dominant negative form. (A) Expression of HA-Erk5^{AEF} in BT474 cells. Cells were infected with pLZR-HA-Erk5^{AEF}-IRES-GFP and analyzed for expression of HA-tagged Erk5^{AEF} by Western blotting with the anti-HA antibody. (B) Comparison of the migration of HA-Erk5^{AEF} between MCF7-Erk5^{AEF} and BT474-Erk5^{AEF}. (C) Confocal immunofluorescence analysis of the distribution of HA-Erk5^{AEF}, Erk1/2, and Erk5 in BT474 or BT474-Erk5^{AEF} cells. Cells plated on glass coverslips were permeabilized and incubated with the antibodies, followed by Cy3-labeled secondary antibodies. Bar, 20 μm. (D) Proliferation of BT474 (closed bars) and BT474-Erk5^{AEF} (open bars) cells. Cells were plated in 24-well dishes in medium containing 10% FBS and then allowed to attach overnight. On the next day, cultures were infected with pLZR-HA-Erk5^{AEF}-IRES-GFP or pLZR-IRES-GFP and switched to the indicated FBS concentrations. Cell proliferation was measured 4 days later by an MTT assay. The results shown are the mean ± SD of quadruplicate measurements of a representative experiment that was repeated at least three times.

activation have generated unclear conclusions. Thus, Erk5 has been shown to be activated in a Ras-independent manner in HeLa cells stimulated with EGF (41). In contrast, EGF- or NGF-induced Erk5 activation in PC12 cells has been reported to depend on Ras (39). In MCF7 cells, expression of RasN17 prevented NRG-induced Ras activation but was unable to prevent the activation of Erk5. Interestingly, Erk1/2 activation in response to NRG was also largely insensitive to the presence of RasN17, suggesting that alternative routes for Erk1/2 activation must exist in these cells. The latter finding was particularly surprising since the Ras route has been linked to Erk1/2 activation by receptor tyrosine kinases in multiple cell lines. However, genetic and biochemical evidence also indicates that activation of the Raf/Erk route by receptor tyrosine kinases may occur through Ras-independent routes. Thus, in flies, coupling of the torso receptor tyrosine kinase to Raf has been reported to occur in a Ras-independent manner (35). In addition, point mutations in the intracellular domain of Ret that prevent Ras activation fail to fully block glia-derived neurotrophic factor-induced Erk1/2 activation (7).

NRG-induced Erk5 activation was prevented by use of the drug U0126. This drug was initially reported as a potent and selective inhibitor of MEK1 and MEK2 (23). More recently, this drug has been shown to prevent EGF-induced Erk5 activation in COS cells (39). Our data confirm that, in addition to its inhibitory effect on Erk1/2, U0126 may also act as an inhibitory drug for the Erk5 pathway by acting on the upstream activating kinases. Furthermore, the dose-response inhibitory effect on Erk5 paralleled that obtained for Erk1/2, raising the important conclusion that data obtained by the use of this drug should take into account this apparent lack of specificity. Because of this, and also due to the fact that no other drug is

Downloaded from http://mcb.asm.org/ on October 23, 2019 by guest

known to specifically inhibit Erk5, attempts to investigate the importance of Erk5 in NRG signal transduction were carried out by the use of a form ($Erk5^{AEF}$) of this kinase in which the TEY sequence in the activation lip was replaced by AEF. Experiments with MCF7 cells expressing the $Erk5^{AEF}$ form showed restricted proliferative responses to NRG with respect to wild-type cells. As expected, expression of this form did not affect upstream signaling events such as ErbB2 or Shc tyrosine phosphorylation or the association between these two proteins. Expression of high levels of $Erk5^{AEF}$ prevented activation of endogenous Erk5 by NRG. However, expression of intermediate levels of $Erk5^{AEF}$ did not block NRG-induced activation of endogenous Erk5. This is interesting, since the latter level of expression was enough to affect NRG-induced proliferation.

A mechanism that may act in concert with interference with Erk5 activation is prevention of nuclear translocation of Erk5 by the $Erk5^{AEF}$ form. Nuclear translocation of Erk5 has been reported to be critical in the induction of nuclear transcription (72). Since Erk5 cytoplasmic retention and oligomerization domains are preserved in the $Erk5^{AEF}$ mutant, it is possible that endogenous Erk5 may be sequestered in the cytosol by its interaction with $Erk5^{AEF}$. In the presence of moderate levels of $Erk5^{AEF}$, interaction between wild-type Erk5 and the mutant form could prevent nuclear translocation of endogenous Erk5 but not its activation by MEK5. Furthermore, this cytoplasmic retention of endogenous Erk5 could facilitate its phosphorylation by MEK5, as indicated by the stronger shifting of Erk5 in the two clones of MCF7 cells expressing intermediate levels of $Erk5^{AEF}$. However, when the levels of $Erk5^{AEF}$ are high enough, the dominant negative form probably titrates cytosolic MEK5, preventing endogenous Erk5 activation. In conclusion, our data, together with those of others (72), indicate that shuttling of Erk5 to the nucleus appears to be as important as activation by phosphorylation for the action of Erk5, as also occurs for the related family members Erk1/2 (9).

Deficient nuclear translocation could explain why significantly less c-Jun induction by NRG was observed in cells transfected with the dominant negative form. This parallels the data obtained in other systems in which the Erk5 route has been shown to mediate c-Jun induction by several treatments (15, 40, 45). While the exact mechanisms by which NRG receptors govern c-Jun levels are unknown, NRG controls transcription factors that regulate c-Jun expression (4, 16, 33). Thus, the promoter of c-Jun contains an Sp1 binding site (16, 33), and NRGs have been shown to stimulate the activity of the Sp1 transcription factor (4). In our study, NRGs activated Sp1 binding activity in both MCF7 and MCF7-$Erk5^{AEF}$ cells; however, in the latter cells a small delay in the activation of Sp1 was observed compared to the effect in MCF7 cells (A. Esparís-Ogando, E. Díaz-Rodríguez, and A. Pandiella, unpublished data). In addition, the MADS box transcription factors of the MEF2 family, which have been shown to participate in c-Jun induction (40), are known targets of the Erk5 kinase. A detailed study of the mechanisms of NRG-induced c-Jun expression that includes the possible participation of these transcription factors and the routes by which they are activated is required.

A finding that may have important therapeutic implications was that Erk5 appeared constitutively active in certain human-derived tumor cell lines. Western blotting of SKBR3 and BT474 cells with anti-Erk5 antibodies detected a form of Erk5 with a retarded mobility analogous to that of NRG-treated samples. Possibilities such as a molecular alteration or deficient dephosphorylation can probably be excluded by the studies on the mechanism of generation of this apparently constitutively active Erk5 form. Thus, immunoprecipitation with the anti-pErk5 antibody indicated that the slower-migrating Erk5 form was dually phosphorylated, suggesting that the retarded migration could be due to the presence of active Erk5. Studies on overall phosphatase activity, as well as on MKP3 and CL100, which have been reported to act as Erk5 phosphatases (39), indicated no evident defects in phosphatase activity. Additional studies pointed to constitutive activation of ErbB receptors as the cause for the presence of permanently active forms of Erk5 in these tumor cell lines. Analysis of the expression of ErbB receptors in these cell lines indicated a correlation among the level of ErbB2, its constitutive phosphorylation status, and the presence of active Erk5. Treatment of BT474 with the ErbB inhibitor DAPH resulted in a change of the slower-migrating Erk5 form to the faster-migrating one. In addition, transfection of MCF7 cells with ErbB2 to increase the endogenous complement of ErbB2 receptors resulted in a shift in the amount of Erk5 to the slower-migrating form. Thus, continuous stimulation of the ErbB2 receptor results in permanent activation of the Erk5 route and probably other Erk pathways (71) that participate in cell proliferation. Interestingly, in A431 cells that overexpress constitutively active EGFR, Erk5 was mostly inactive under resting conditions. Since the estimated levels of EGFR in A431 cells is analogous to the levels of the other ErbB receptors (particularly ErbB2) in BT474 and SKBR3, it is possible that the differences in the level of activation of Erk5 may be due to stronger coupling of ErbB2, ErbB3, or ErbB4 to the Erk5 pathway than the EGFR.

In summary, our data point to Erk5 as an important MAPK in the regulation of NRG-induced cell proliferation. Because of its constitutive activation and role in the growth of certain tumor cells, it may be important to define specific drugs that target the Erk5 pathway. Efforts in that direction are being carried out in our laboratory.

ACKNOWLEDGMENTS

We acknowledge the different scientists mentioned in this paper for supplying the reagents used. We particularly thank X. Bustelo and E. Santos for continuous discussions and encouragement.

We acknowledge funding from the European Community, the Fundación Ramón Areces, and the Spanish Ministry of Education and Culture. A.E.-O. was supported by a postdoctoral contract from the Spanish Ministry of Education and Culture. E.D.-R. and L.Y. were supported by a predoctoral fellowship from the same ministry.

REFERENCES

1. **Abe, J., M. Kusuhara, R. J. Ulevitch, B. C. Berk, and J. D. Lee.** 1996. Big mitogen-activated protein kinase 1 (BMK1) is a redox-sensitive kinase. J. Biol. Chem. **271:**16586–16590.
2. **Abe, J., M. Takahashi, M. Ishida, J. D. Lee, and B. C. Berk.** 1997. c-Src is required for oxidative stress-mediated activation of big mitogen-activated protein kinase 1. J. Biol. Chem. **272:**20389–20394.
3. **Alimandi, M., L.-M. Wang, D. Bottaro, C.-C. Lee, A. Kuo, M. Frankel, P. Fedi, C. Tang, M. Lippman, and J. H. Pierce.** 1997. Epidermal growth factor and betacellulin mediate signal transduction through co-expressed ErbB2 and ErbB3 receptors. EMBO J. **16:**5608–5617.
4. **Alroy, I., L. Soussan, R. Seger, and Y. Yarden.** 1999. Neu differentiation factor stimulates phosphorylation and activation of the Sp1 transcription factor. Mol. Cell. Biol. **19:**1961–1972.
5. **Ausubel, F. M., R. Brent, R. E. Kingston, D. D. Moore, J. G. Seidman, J. A.**

Downloaded from http://mcb.asm.org/ on October 23, 2019 by guest

Smith, and K. Struhl. 1987. Current protocols in molecular biology. John Wiley & Sons, Inc., New York, N.Y.
6. **Ballinger, M. D., J. T. Jones, J. A. Lofgren, W. J. Fairbrother, R. W. Akita, M. X. Sliwkowski, and J. A. Wells.** 1998. Selection of heregulin variants having higher affinity for the ErbB3 receptor by monovalent phage display. J. Biol. Chem. **273:**11675–11684.
7. **Besset, V., R. P. Scott, and C. F. Ibanez.** 2000. Signaling complexes and protein-protein interactions involved in the activation of the Ras and phosphatidylinositol 3-kinase pathways by the c-Ret receptor tyrosine kinase. J. Biol. Chem. **275:**39159–39166.
8. **Britsch, S., L. Li, S. Kirchhoff, F. Theuring, V. Brinkmann, C. Birchmeier, and D. Riethmacher.** 1998. The ErbB2 and ErbB3 receptors and their ligand, neuregulin-1, are essential for development of the sympathetic nervous system. Genes Dev. **12:**1825–1836.
9. **Brunet, A., D. Roux, P. Lenormand, S. Dowd, S. Keyse, and J. Pouyssegur.** 1999. Nuclear translocation of p42/p44 mitogen-activated protein kinase is required for growth factor-induced gene expression and cell cycle entry. EMBO J. **18:**664–674.
10. **Buchdunger, E., U. Trinks, H. Mett, U. Regenass, M. Muller, T. Meyer, E. McGlynn, L. A. Pinna, P. Traxler, and N. B. Lydon.** 1994. 4,5-Dianilinophthalimide: a protein-tyrosine kinase inhibitor with selectivity for the epidermal growth factor receptor signal transduction pathway and potent in vivo antitumor activity. Proc. Natl. Acad. Sci. USA **91:**2334–2338.
11. **Burden, S., and Y. Yarden.** 1997. Neuregulins and their receptors: a versatile signalling module in organogenesis and oncogenesis. Neuron **18:**847–855.
12. **Cabrera, N., E. Díaz-Rodríguez, E. Becker, D. M. Zanca, and A. Pandiella.** 1996. TrkA receptor ectodomain cleavage generates a tyrosine-phosphorylated cell-associated fragment. J. Cell Biol. **132:**427–436.
13. **Chang, L., and M. Karin.** 2001. Mammalian MAP kinase signalling cascades. Nature **410:**37–40.
14. **Chao, T. H., M. Hayashi, R. I. Tapping, Y. Kato, and J. D. Lee.** 1999. MEKK3 directly regulates MEK5 activity as part of the big mitogen-activated protein kinase 1 (BMK1) signaling pathway. J. Biol. Chem. **274:**36035–36038.
15. **Chiariello, M., M. J. Marinissen, and J. S. Gutkind.** 2000. Multiple mitogen-activated protein kinase signaling pathways connect the Cot oncoprotein to the c-*jun* promoter and to cellular transformation. Mol. Cell. Biol. **20:**1747–1758.
16. **Coso, O. A., S. Montaner, C. Fromm, J. C. Lacal, R. Prywes, H. Teramoto, and J. S. Gutkind.** 1997. Signaling from G protein-coupled receptors to the c-jun promoter involves the MEF2 transcription factor. Evidence for a novel c-jun amino-terminal kinase-independent pathway. J. Biol. Chem. **272:**20691–20697.
17. **Daly, J. M., C. B. Jannot, R. R. Beerli, D. Graus-Porta, F. G. Maurer, and N. E. Hynes.** 1997. Neu differentiation factor induces ErbB2 down-regulation and apoptosis of ErbB2-overexpressing breast tumor cells. Cancer Res. **57:**3804–3811.
18. **Daly, J. M., M. A. Olayioye, A. M. Wong, R. Neve, H. A. Lane, F. G. Maurer, and N. E. Hynes.** 1999. NDF/heregulin-induced cell cycle changes and apoptosis in breast tumour cells: role of PI3 kinase and p38 MAP kinase pathways. Oncogene **18:**3440–3451.
19. **Daly, R. J.** 1999. Take your partners, please—signal diversification by the erbB family of receptor tyrosine kinases. Growth Factors **16:**255–263.
20. **English, J. M., G. Pearson, R. Baer, and M. H. Cobb.** 1998. Identification of substrates and regulators of the mitogen-activated protein kinase ERK5 using chimeric protein kinases. J. Biol. Chem. **273:**3854–3860.
21. **English, J. M., G. Pearson, T. Hockenberry, L. Shivakumar, M. A. White, and M. H. Cobb.** 1999. Contribution of the ERK5/MEK5 pathway to Ras/Raf signaling and growth control. J. Biol. Chem. **274:**31588–31592.
22. **Esparís-Ogando, A., E. Díaz-Rodríguez, and A. Pandiella.** 1999. Signalling-competent truncated forms of ErbB2 in breast cancer cells: differential regulation by protein kinase C and phosphatidylinositol 3-kinase. Biochem. J. **344:**339–348.
23. **Favata, M. F., K. Y. Horiuchi, E. J. Manos, A. J. Daulerio, D. A. Stradley, W. S. Feeser, D. E. Van Dyk, W. J. Pitts, R. A. Earl, F. Hobbs, R. A. Copeland, R. L. Magolda, P. A. Scherle, and J. M. Trzaskos.** 1998. Identification of a novel inhibitor of mitogen-activated protein kinase kinase. J. Biol. Chem. **273:**18623–18632.
24. **Fiddes, R. J., P. W. Janes, S. P. Sivertsen, R. L. Sutherland, E. A. Musgrove, and R. J. Daly.** 1998. Inhibition of the MAP kinase cascade blocks heregulin-induced cell cycle progression in T-47D human breast cancer cells. Oncogene **16:**2803–2813.
25. **Fukuhara, S., M. J. Marinissen, M. Chiariello, and J. S. Gutkind.** 2000. Signaling from G protein-coupled receptors to ERK5/Big MAPK 1 involves Gαq and Gα12/13 families of heterotrimeric G proteins. Evidence for the existence of a novel ras and rho-independent pathway. J. Biol. Chem. **275:**21730–21736.
26. **Garrington, T. P., and G. L. Johnson.** 1999. Organization and regulation of mitogen-activated protein kinase signaling pathways. Curr. Opin. Cell Biol. **11:**211–218.
27. **Gonzalez, F. A., A. Seth, D. L. Raden, D. S. Bowman, F. S. Fay, and R. J. Davis.** 1993. Serum-induced translocation of mitogen-activated protein kinase to the cell surface ruffling membrane and the nucleus. J. Cell Biol. **122:**1089–1101.
28. **Grasso, A. W., D. Wen, C. M. Miller, J. S. Rhim, T. G. Pretlow, and H. J. Kung.** 1997. ErbB kinases and NDF signaling in human prostate cancer cells. Oncogene **15:**2705–2716.
29. **Graus-Porta, D., R. R. Beerli, J. M. Daly, and N. E. Hynes.** 1997. ErbB-2, the preferred heterodimerization partner of all ErbB receptors, is a mediator of lateral signaling. EMBO J. **16:**1647–1655.
30. **Gullick, W. J., S. B. Love, C. Wright, D. M. Barnes, B. Gusterson, A. L. Harris, and D. G. Altman.** 1991. c-erbB-2 protein overexpression in breast cancer is a risk factor in patients with involved and uninvolved lymph nodes. Br. J. Cancer **63:**434–438.
31. **Gutkind, J. S.** 1998. Cell growth control by G protein-coupled receptors: from signal transduction to signal integration. Oncogene **17:**1331–1342.
32. **Guy, P. M., J. V. Platko, L. C. Cantley, R. A. Cerione, and K. L. Carraway III.** 1994. Insect cell-expressed $p180^{erbB3}$ possesses an impaired tyrosine kinase activity. Proc. Natl. Acad. Sci. USA **91:**8132–8136.
33. **Han, T.-H., and R. Prywes.** 1995. Regulatory role of MEF2D in serum induction of the c-*jun* promoter. Mol. Cell. Biol. **15:**2907–2915.
34. **Holmes, W. E., M. X. Sliwkowski, R. W. Akita, W. J. Henzel, J. Lee, J. W. Park, D. Yansura, N. Abadi, H. Raab, G. D. Lewis, H. M. Shepard, W. J. Kuang, W. I. Wood, D. V. Goeddel, and R. L. Vandlen.** 1992. Identification of heregulin, a specific activator of $p185^{erbB2}$. Science **256:**1205–1210.
35. **Hou, X. S., T. B. Chou, M. B. Melnick, and N. Perrimon.** 1995. The torso receptor tyrosine kinase can activate Raf in a Ras-independent pathway. Cell **81:**63–71.
36. **Hynes, N. E., and D. F. Stern.** 1994. The biology of *erbB-2/neu*/HER2 and its role in cancer. Biochim. Biophys. Acta **1198:**165–184.
37. **Ip, Y. T., and R. J. Davis.** 1998. Signal transduction by the c-Jun N-terminal kinase (JNK)—from inflammation to development. Curr. Opin. Cell Biol. **10:**205–219.
38. **Jones, J. T., M. D. Ballinger, P. I. Pisacane, J. A. Lofgren, V. D. Fitzpatrick, W. J. Fairbrother, J. A. Wells, and M. X. Sliwkowski.** 1998. Binding interaction of the heregulinβ egf domain with ErbB3 and ErbB4 receptors assessed by alanine scanning mutagenesis. J. Biol. Chem. **273:**11667–11674.
39. **Kamakura, S., T. Moriguchi, and E. Nishida.** 1999. Activation of the protein kinase ERK5/BMK1 by receptor tyrosine kinases. Identification and characterization of a signaling pathway to the nucleus. J. Biol. Chem. **274:**26563–26571.
40. **Kato, Y., V. V. Kravchenko, R. I. Tapping, J. Han, R. J. Ulevitch, and J. D. Lee.** 1997. BMK1/ERK5 regulates serum-induced early gene expression through transcription factor MEF2C. EMBO J. **16:**7054–7066.
41. **Kato, Y., R. I. Tapping, S. Huang, M. H. Watson, R. J. Ulevitch, and J. D. Lee.** 1998. Bmk1/Erk5 is required for cell proliferation induced by epidermal growth factor. Nature **395:**713–716.
42. **Lange-Carter, C. A., and G. L. Johnson.** 1994. Ras-dependent growth factor regulation of MEK kinase in PC12 cells. Science **265:**1458–1461.
43. **Lee, J. D., R. J. Ulevitch, and J. Han.** 1995. Primary structure of BMK1: a new mammalian map kinase. Biochem. Biophys. Res. Commun. **213:**715–724.
44. **Lenormand, P., C. Sardet, G. Pages, G. L'Allemain, A. Brunet, and J. Pouyssegur.** 1993. Growth factors induce nuclear translocation of MAP kinases (p42mapk and p44mapk) but not of their activator MAP kinase kinase (p45mapkk) in fibroblasts. J. Cell Biol. **122:**1079–1088.
45. **Marinissen, M. J., M. Chiariello, M. Pallante, and J. S. Gutkind.** 1999. A network of mitogen-activated protein kinases links G protein-coupled receptors to the c-*jun* promoter: a role for c-Jun NH_2-terminal kinase, p38s, and extracellular signal-regulated kinase 5. Mol. Cell. Biol. **19:**4289–4301.
46. **Marshall, C.** 1999. How do small GTPase signal transduction pathways regulate cell cycle entry? Curr. Opin. Cell Biol. **11:**732–736.
47. **Marshall, C. J.** 1999. Small GTPases and cell cycle regulation. Biochem. Soc. Trans. **27:**363–370.
48. **Massagué, J., and A. Pandiella.** 1993. Membrane-anchored growth factors. Annu. Rev. Biochem. **62:**515–541.
49. **Minden, A., A. Lin, M. McMahon, C. Lange-Carter, B. Derijard, R. J. Davis, G. L. Johnson, and M. Karin.** 1994. Differential activation of ERK and JNK mitogen-activated protein kinases by Raf-1 and MEKK. Science **266:**1719–1723.
50. **Olayioye, M. A., D. Graus-Porta, R. R. Beerli, J. Rohrer, B. Gay, and N. E. Hynes.** 1998. ErbB-1 and ErbB-2 acquire distinct signaling properties dependent upon their dimerization partner. Mol. Cell. Biol. **18:**5042–5051.
51. **Peles, E., S. S. Bacus, R. A. Koski, H. S. Lu, D. Wen, S. G. Ogden, R. B. Levy, and Y. Yarden.** 1992. Isolation of the Neu/HER-2 stimulatory ligand: a 44 kd glycoprotein that induces differentiation of mammary tumor cells. Cell **69:**205–216.
52. **Pinkas-Kramarski, R., M. Shelly, S. Glathe, B. J. Ratzkin, and Y. Yarden.** 1996. Neu differentiation factor/neuregulin isoforms activate distinct receptor combinations. J. Biol. Chem. **271:**19029–19032.
53. **Pinkas-Kramarski, R., M. Shelly, B. C. Guarino, L. M. Wang, L. Lyass, I. Alroy, M. Alimandi, A. Kuo, J. D. Moyer, S. Lavi, M. Eisenstein, B. J. Ratzkin, R. Seger, S. S. Bacus, J. H. Pierce, G. C. Andrews, Y. Yarden, and M. Alamandi.** 1998. ErbB tyrosine kinases and the two neuregulin families

Downloaded from http://mcb.asm.org/ on October 23, 2019 by guest

constitute a ligand-receptor network. Mol. Cell. Biol. **18:**6090–6101.
54. **Riese, D. J., II, and D. F. Stern.** 1998. Specificity within the EGF family/ErbB receptor family signaling network. Bioessays **20:**41–48.
55. **Riethmacher, D., E. Sonnenberg-Riethmacher, V. Brinkmann, T. Yamaai, G. R. Lewin, and C. Birchmeier.** 1997. Severe neuropathies in mice with targeted mutations in the ErbB3 receptor. Nature **389:**725–730.
56. **Robinson, M. J., and M. H. Cobb.** 1997. Mitogen-activated protein kinase pathways. Curr. Opin. Cell Biol. **9:**180–186.
57. **Samanta, A., C. M. LeVea, W. C. Dougall, X. Quian, and M. I. Greene.** 1994. Ligand and p185$^{c\text{-}neu}$ density govern receptor interactions and tyrosine kinase activation. Proc. Natl. Acad. Sci. USA **91:**1711–1715.
58. **Schaeffer, H. J., and M. J. Weber.** 1999. Mitogen-activated protein kinases: specific messages from ubiquitous messengers. Mol. Cell. Biol. **19:**2435–2444.
59. **Schönwasser, D. C., R. M. Marais, C. J. Marshall, and P. J. Parker.** 1998. Activation of the mitogen-activated protein kinase/extracellular signal-regulated kinase pathway by conventional, novel and atypical protein kinase C isotypes. Mol. Cell. Biol. **18:**790–798.
60. **Shields, J. M., K. Pruitt, A. McFall, A. Shaub, and C. J. Der.** 2000. Understanding Ras: 'it ain't over 'til it's over'. Trends Cell Biol. **10:**147–154.
61. **Sibilia, M., J. P. Steinbach, L. Stingl, A. Aguzzi, and E. F. Wagner.** 1998. A strain-independent postnatal neurodegeneration in mice lacking the EGF receptor. EMBO J. **17:**719–731.
62. **Siegel, P. M., E. D. Ryan, R. D. Cardiff, and W. J. Muller.** 1999. Elevated expression of activated forms of Neu/ErbB-2 and ErbB-3 are involved in the induction of mammary tumors in transgenic mice: implications for human breast cancer. EMBO J. **18:**2149–2164.
63. **Slamon, D. J., G. M. Clark, S. G. Wong, W. J. Levin, A. Ullrich, and W. L. McGuire.** 1987. Human breast cancer: correlation of relapse and survival with amplification of the HER-2/neu oncogene. Science **235:**177–182.
64. **Slamon, D. J., W. Godolphin, L. A. Jones, J. A. Holt, S. G. Wong, D. E. Keith, W. J. Levin, S. G. Stuart, J. Udove, A. Ullrich, et al.** 1989. Studies of the HER-2/neu proto-oncogene in human breast and ovarian cancer. Science **244:**707–712.
65. **Tzahar, E., R. Pinkas-Kramarski, J. D. Moyer, L. N. Klapper, I. Alroy, G. Levkowitz, M. Shelly, S. Henis, M. Eisenstein, B. J. Ratzkin, M. Sela, G. C. Andrews, and Y. Yarden.** 1997. Bivalence of EGF-like ligands drives the ErbB signaling network. EMBO J. **16:**4938–4950.
66. **Tzahar, E., and Y. Yarden.** 1998. The ErbB-2/HER2 oncogenic receptor of adenocarcinomas: from orphanhood to multiple stromal ligands. Biochim. Biophys. Acta **1377:**M25–M37.
67. **Ullrich, A., and J. Schlessinger.** 1990. Signal transduction by receptors with tyrosine kinase activity. Cell **61:**203–212.
68. **van der Geer, P., T. Hunter, and R. A. Lindberg.** 1994. Receptor protein tyrosine kinases and their signal transduction pathways. Annu. Rev. Cell Biol. **10:**251–337.
69. **Wallasch, C., F. U. Weiss, G. Niederfellner, B. Jallal, W. Issing, and A. Ullrich.** 1995. Heregulin-dependent regulation of HER2/neu oncogenic signaling by heterodimerization with HER3. EMBO J. **14:**4267–4275.
70. **Widmann, C., S. Gibson, M. B. Jarpe, and G. L. Johnson.** 1999. Mitogen-activated protein kinase: conservation of a three-kinase module from yeast to human. Physiol. Rev. **79:**143–180.
71. **Wu, C. J., X. Qian, and D. M. O'Rourke.** 1999. Sustained mitogen-activated protein kinase activation is induced by transforming erbB receptor complexes. DNA Cell Biol. **18:**731–741.
72. **Yan, C., H. Luo, J. D. Lee, J. Abe, and B. C. Berk.** 2001. Molecular cloning of mouse ERK5/BMK1 splice variants and characterization of ERK5 functional domains. J. Biol. Chem. **276:**10870–10878.
73. **Yan, C., M. Takahashi, M. Okuda, J. D. Lee, and B. C. Berk.** 1999. Fluid shear stress stimulates big mitogen-activated protein kinase 1 (BMK1) activity in endothelial cells. Dependence on tyrosine kinases and intracellular calcium. J. Biol. Chem. **274:**143–150.
74. **Yang, C. C., O. I. Ornatsky, J. C. McDermott, T. F. Cruz, and C. A. Prody.** 1998. Interaction of myocyte enhancer factor 2 (MEF2) with a mitogen-activated protein kinase, ERK5/BMK1. Nucleic Acids Res. **26:**4771–4777.
75. **Zecevic, M., A. D. Catling, S. T. Eblen, L. Renzi, J. C. Hittle, T. J. Yen, G. J. Gorbsky, and M. J. Weber.** 1998. Active MAP kinase in mitosis: localization at kinetochores and association with the motor protein CENP-E. J. Cell Biol. **142:**1547–1558.
76. **Zhou, G., Z. Q. Bao, and J. E. Dixon.** 1995. Components of a new human protein kinase signal transduction pathway. J. Biol. Chem. **270:**12665–12669.
77. **Zwijsen, R. M., R. Klompmaker, E. B. Wientjens, P. M. Kristel, B. van der Burg, and R. J. Michalides.** 1996. Cyclin D1 triggers autonomous growth of breast cancer cells by governing cell cycle exit. Mol. Cell. Biol. **16:**2554–2560.

Downloaded from http://mcb.asm.org/ on October 23, 2019 by guest